# DEVELOPING A FOURIER-TRANSFORM INFRARED (FT-IR) SPECTROSCOPY CLASSIFICATION TOOL TO IDENTIFY COMMON BEACH PLASTICS ON HAWAI'I ISLAND

A THESIS SUBMITTED TO THE GRADUATE DIVISION OF THE UNIVERSITY OF HAWAI'I AT HILO IN PARTIAL FULFILLMENT OF THE REQUIREMENTS FOR THE DEGREE OF

MASTER OF SCIENCE

IN

TROPICAL CONSERVATION BIOLOGY AND ENVIRONMENTAL SCIENCE

DECEMBER 2021

By

Kathryn L. Strong

Thesis Committee:

Mazen Hamad, Chairperson
Karla McDermid, Grady Weyenberg

Keywords: Machine Learning, Marine Debris, Infrared Spectroscopy, Polymers

**Acknowledgments**

Mahalo to my advisor Dr. Mazen Hamad for providing overall project guidance, technical support, and the freedom to fully pursue my research interest. Thank you to my committee members Dr. Karla McDermid and Dr. Grady Weyenberg for their time, manuscript edits, and expertise. I would also like to thank the University of Hawai‘i at Hilo Chemistry Department for providing access to instrumentation, resources, and laboratory space the past few years. A big mahalo to the University of Hawai‘i at Hilo Research Council and The American Association of University Women for providing the project funding and tuition support. I would like to sincerely thank the Tropical Conservation Biology and Environmental Science Program professors and staff. Thank you to Hawai‘i Wildlife Fund and Algalita Marine Research Foundation for project support. Additionally, I would like to thank the University of Hawai‘i at Hilo Marine Science Department for their marine debris expertise and field equipment loan. A special thank you to the following people for sharing their knowledge and service, and for assisting me in achieving my research goals: Dr. Steven Colbert, Dr. Jon-Pierre Michaud, Megan Lamson, Dr. Rebecca Ostertag, Dr. Tim Grabowski, Dr. Jolene Sutton, Dawn Namahoe Sidman, Captain Charles Moore, Richard Masse, Etta Karth, Erica Honda, Eszter Collier, Ashley Pugh, Dr. Marina Karides, Dr. Matthew Platz, and Dr. Matthew Knope. Finally, a big thank you to my parents and partner for all the support and encouragement.

**Abstract**

Many studies rely on Fourier-transform infrared spectroscopy (FT-IR) to identify the plastic polymer types of micro to macro plastics collected from marine and coastal environments. FT-IR research predominantly uses pre-installed reference library software to identify unknown plastic polymer types. However, plastic recovered from the outdoor environment is often altered by heat and ultraviolet light, which changes its chemical composition and consequently its FT-IR spectrum. Reference library limitations make proper identification of weathered plastic spectra challenging. In the following study, various separation and machine learning techniques were developed and evaluated to create a FT-IR beach plastic classification tool. The multivariate classification algorithm of Principal Component Analysis (PCA) served as the model framework for the tool, and two PCA models were developed and tested. The first PCA model served as a baseline and was built based on the spectra of known unweathered plastic polymers, referred to as standards. After five preprocessing techniques were applied to the spectra, the first PCA model separated the 96 standards into eight distinct groups within the modeled 99% confidence limit. Initially, the second PCA model, composed of the same standards with the addition of unknown beach plastics calibrated into the model, was unable to separate plastic polymer types into eight groups. The second PCA model was then modified to reduce the number of plastic polymer standards and beach plastics to the three most common beach plastic types sampled. Polyethylene (PE), polypropylene (PP) and polystyrene (PS) served as the framework for the new model, which classified 77% of beach plastics sampled, compared to the first PCA model, which classified 42% of all beach plastic samples. As a result of numerous metrics and

preprocessing applications, developing a robust identification tool for common beach plastics remains a challenge. The results indicate the new PCA model provided an improvement in plastic polymer classification and holds promise to serve as a tool to identify weathered plastics found not only on Hawai'i Island beaches but worldwide.

**Table of contents**

**List of Tables**

**List of Figures**

**List of Abbreviations**

ABS: acrylonitrile butadiene styrene

AMTIR: amorphous material transmitting infrared radiation

ATR: attenuated total reflectance

CI: carbonyl index

FT-IR: Fourier-transform infrared spectroscopy

HDPE: high-density polyethylene

IR: infrared

LDPE: low-density

LV: Latent Variable

Nylon: nylon 6.6 and nylon 6

PC: Principal Component

PCA: Principal Component Analysis

PE: polyethylene

PET: polyethylene terephthalate

PLS-DA: Partial Least Squares Discriminant Analysis

PP: polypropylene

PS: polystyrene

PVC: polyvinyl chloride

SAUB: specified area under band

TPE: thermoplastic elastomer

## Introduction

Approximately 12,000 million metric tons of plastic waste is predicted to fill our natural environment and landfills by 2050. The rate at which plastic is recovered from our environment is far lower than the rate at which plastic is produced (Geyer et al. 2017). This gap leads to the accumulation of plastic, not only on land and in fresh water, but also in oceans (Eriksen et al. 2014).

Every minute, the equivalent of a dump truck full of plastic (33 thousand pounds of plastic) enters the ocean—totaling eight million metric tons of plastic a year (Jambeck et al. 2015). The Hawaiian Archipelago is impacted by marine plastic debris because of its proximity to the North Pacific Subtropical Eastern Accumulation Zone and Subtropical Convergence Zone, where marine plastic collects (Jia et al. 2011, Carson 2013). Ocean currents and northeasterly trade winds then wash this plastic—in various stages of degradation—onto the islands.

The southernmost island, Hawai'i, accumulates high levels of plastic debris especially on south beaches because of the direction of ocean currents and local eddies. Plastic marine debris harms a high diversity of species and ecosystems on Hawai'i Island (Carson et al. 2013, Clukey et al. 2017). Plastic is composed of many harmful additives and adsorbs toxicants while in the ocean. Plastic leaches these toxicants as it degrades (Andrady 1990, Rochman et al. 2013). Increased ultraviolet exposure and heat buildup cause beached plastic to degrade faster and emit more greenhouse gases than plastic in the marine environment (Barnes et al. 2009, Royer et al. 2018).

Each plastic type has a unique molecular structure, density, chemical absorption, and degradation process and rate (Fotopoulou et al. 2015, Gewert et al. 2015). Once a plastic's chemical composition is determined, its potential source and hazards to the coastal ecosystem can be assessed. Resin identification codes, numbers 1-7, are imprinted on common types of plastics. These codes represent the plastic polymers that make up the product. As plastic degrades and fragments, its resin identification code can become unreadable. Many plastic types are manufactured without a resin code, making plastic identification difficult.

Infrared (IR) spectroscopy, specifically Fourier-transform infrared spectroscopy (FT-IR), has been used in studies to identify unknown plastic marine debris around the globe (Corcoran et al. 2009, Carson et al. 2011, Young and Elliott 2016, Munari et al. 2017, Syakti et al. 2017, Lebreton et al. 2018, Jung et al. 2018). Yet these studies are limited, and FT-IR plastic marine debris studies on Hawai'i Island are even fewer (Carson et al. 2011, Young and Elliott 2016). Nearly all the studies used reference libraries developed from unweathered plastic samples to identify plastic polymer types. Using laboratory libraries makes the accurate identification of beach plastic polymer types difficult; using such libraries could lead to inaccurate identifications (Jung et al. 2018).

FT-IR spectroscopy research identifying plastic polymer types on Hawai'i Island has been restricted to Kamilo and Waikapuna beaches, located on the southeast side of the island (Carson et al. 2011, Young and Elliott 2016). Until now, there has never been an FT-IR spectroscopy island-wide study of the plastic polymer types found on Hawai'i Island's beaches. Nor has a FT-IR plastic polymer classification tool been created from beach plastics to identify plastics in the environment.

Identifying the plastic polymer types of beach plastics and their degradation status can lead to a better understanding of the plastics' origins, degradation processes, and biological hazards. No other study has calibrated degraded beach samples into an analysis model.

The goal of creating a FT-IR plastic classification tool was to improve the process of identifying degraded and non-degraded beach plastic polymer types by making the process simpler, less time-consuming, and more accurate than using software libraries or self-identification, resulting in more robust identification. The hope is that the FT-IR plastic classification tool will assist resource managers and lawmakers in prioritizing beach plastic removal and land-based mitigation efforts worldwide.

*Research objectives*

The plastic classification tool is designed to serve as a reference for researchers to identify marine plastics worldwide. This research is unique because the researcher developed a classification tool built from plastic polymers collected from the natural environment. Researchers conducting previous FT-IR spectroscopy plastic marine debris studies used reference libraries made up of IR spectra from pure laboratory samples of plastics. These libraries of pure, unweathered samples are not the best resource in identifying the plastic polymer type of beach plastics because the weathering of plastics affects their IR spectra. If weathering is not taken into account in the library, misidentification can result. For the classification tool developed from this study, the FT-IR spectra of eight plastic polymer types were used including unweathered and weathered samples recovered from beaches and recycling bins, as well as pure samples from plastic manufacturing companies. The use of FT-IR spectra

from a variety of samples for each plastic type was thought to provide a more accurate and robust tool to identify common plastics found on Hawaiian beaches.

The research objectives were: (1) Use FT-IR spectroscopy to create a classification tool composed of eight common types of beach plastic, serving as plastic standards for the tool. The framework of the tool was developed with unweathered, known plastic polymers. (2) Explore preprocessing methods and multivariate analysis methods to build a statistically robust plastic identification model. (3) Use the transmittance bands identification method to identify plastic polymer types of up to 400 micro to macro beach plastic samples from eight Hawai'i Island beaches. (4) Assess the presence of outside weathering for 350 plastic polymer samples collected from eight Hawai'i Island beaches. (5) Calibrate 96 identified beach plastic polymer samples from eight beaches into the identification tool model, developing the final classification tool. (6) Assess the accuracy of the final classification tool by determining the percentage of beach plastic samples that was validated and correctly classified with the model.

*Hypotheses*

This research tested the following hypotheses:

1. The plastic polymer standards can be separated into eight groups according to their plastic polymer type, through unsupervised machine learning techniques.
2. The beaches with the highest proportion of ocean-based plastics (low polymer diversity) have plastics with the largest differences between their surface spectra and their inside (subsurface) spectra.
3. There is a significant correlation between the presence of outside weathering and the

presence of a carbonyl peak within the surface spectra of polyethylene and polystyrene beach samples.

## Methods

The research developed a FT-IR spectroscopy plastic polymer classification tool. The inputs into the tool were thoroughly tested to build a statistically robust model. The tool identified eight common types of beach plastic. The tool was piloted to identify unknown plastic samples found on eight Hawai'i Island beaches.

### *Sourcing standards*

Six of the eight common beach plastics were recovered from recycling bins. These six types and their resin identification codes were the following: polyethylene terephthalate (PET) resin identification #1, high-density polyethylene (HDPE) resin identification #2, polyvinyl chloride (PVC) resin identification #3, low-density polyethylene (LDPE) resin identification #4, polypropylene (PP) resin identification #5, and polystyrene (PS) resin identification #6. The remaining common beach plastics did not have resin identification codes and were sourced from plastic manufacturing companies. These plastic polymer types were: nylon 6.6 (nylon), nylon 6 (nylon), acrylonitrile butadiene styrene (ABS), and thermoplastic elastomer (TPE). High-density and low-density polyethylene were combined into one class, and nylon 6.6 and nylon 6 were also combined into one class. Previous FT-IR research showed that the two nylons and the two polyethylenes could not be separated without further analysis (Verleye et al. 2001, Jung et al. 2018).

*Plastic polymer types and chemical structures*

Each of the common beach plastics have a known molecular structure that signifies its plastic polymer type. The chemical structures are illustrated (Tab. 1) with their corresponding plastic polymer type and resin identification code or manufactured source (Jung et al. 2018).

**Table 1.** Chemical Structures, & Resin Code or Manufacturing Source of Common Beach Plastics

| **Plastic Polymer Type** | **Resin Code or Manufacture** | **Chemical Structure (Jung et al. 2018)** |
|---|---|---|
| Polyethylene terephthalate (PET) | 1 | 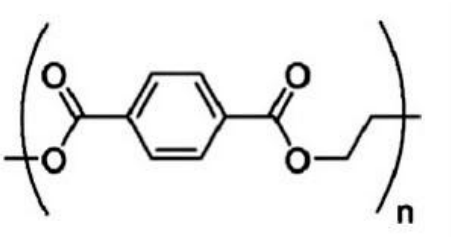 |
| Polyethylene (PE) | 2 & 4 | 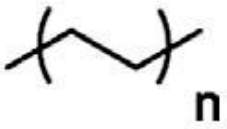 |
| Polyvinyl chloride (PVC) | 3 | 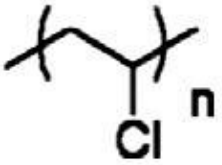 |
| Polypropylene (PP) | 5 | 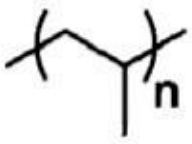 |

| | | |
|---|---|---|
| Polystyrene (PS) | 6 | 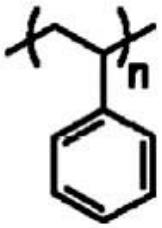 |
| Nylon 6.6, nylon 6 (nylon) | DuPont | 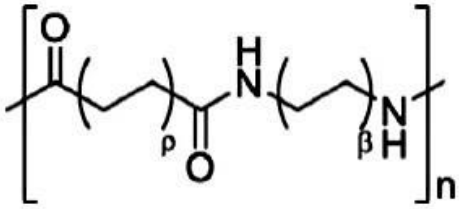 |
| Acrylonitrile butadiene styrene (ABS) | DuPont | 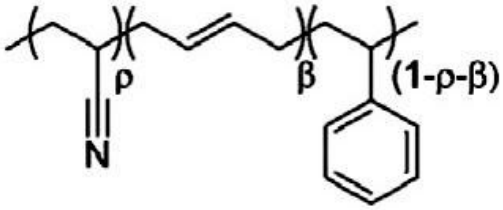 |

*Analyzing standards with FT-IR*

Five samples of each of the eight plastic polymer types were obtained. The types were analyzed using a FT-IR spectrophotometer. Five samples of each of the eight common types of beach plastic were analyzed three times, creating 120 spectra. Analysis was performed using a Shimadzu IRAffinity-1 FT-IR instrument set at a 32 scan with approximately a 2 wavenumber $cm^{-1}$ resolution from a range of 650 $cm^{-1}$ to 4000 $cm^{-1}$. FT-IR spectroscopy determines plastic polymer type by irradiating a sample with infrared light, which produces a spectrum analogous to a "fingerprint" for each plastic type. This fingerprint is based on the percentage of light at each wavenumber transmitted through the sample. The light not transmitted through the sample is

absorbed by the sample.

Traditional FT-IR spectroscopy requires light to pass through the sample. This normally requires solid samples to be ground into a powder or dissolved in a solvent. This study used the attenuated total reflectance (ATR) method for measuring IR spectra. In the ATR method, the plastic sample was pressed in its original form against a zinc selenide (ZnSe) crystal. The crystal-sample interface reflects the IR light and generates an evanescent wave that penetrates the sample. The sample absorbs the evanescent light at particular wavenumbers, resulting in a fingerprint pattern. The ATR method was selected as a result of it producing high quality FT-IR spectra, and being faster and easier to perform than the traditional transmission-based FT-IR method.

*Data collection and beach sampling*

Beach plastic was collected from eight Hawai'i Island beaches. Four beaches were sampled on the island's windward side and four on the leeward side. The windward beaches were Pololū Valley, Hilo Bay, Ka'alu'alu Bay, and Kaulana Bay. The leeward beaches were Pine Trees, Old Kona Airport, North Miloli'i, and South Miloli'i. All eight beaches were sampled during one sampling event. A common standing-stock beach survey sampling method was used. This method consisted of sampling the top sediment layer from the surface down to 3 cm deep, within three 1 $m^2$ quadrats spaced evenly along the high spring-tide/high strandline (McDermid and McMullen 2004; Costa et al. 2010; Jayasiri et al. 2013; Shim et al. 2018). All plastics ranging from 2 mm to 1 m in diameter that lay within the 1 $m^2$ quadrats were collected and analyzed.

Google Earth Pro 9.0 was used to obtain a length measurement for each beach prior to

sampling. Each beach was divided into four sections of equal lengths. A transect was laid on the high spring-tide/high strandline. The sediment type was noted and photographed. A 1 $m^2$ quadrat was laid at each of the three predetermined points on the transect line. A sample was obtained in the sediment of each of these three quadrats. A garden trowel was used to scoop the top 3 cm of sediment within the quadrat. The sediment was placed in a 1-L plastic container. Each 1-L sediment sample was collected and sieved through a 4-mm sieve and then through a 2-mm sieve. Any visible plastic pieces were removed and collected. The remaining sediment on top of the 2-mm sieve was placed into a 43 x 35 cm container filled with 250 ml of ocean water. Plastic material was collected from the water's surface and the sinking sediment was combed through for plastics. A total of 4-L of sediment was collected for each quadrat; the process was repeated four times at each quadrat and 12 times at each beach.

For beaches that resulted in < 50 plastic samples after the common standing-stock beach survey sampling method, an additional belt transect sampling method was performed. The belt transect method was also performed instead of the common standing-stock beach survey sampling method when sieving was not an option. The belt transect method was performed by laying a transect line on the high spring-tide/high strandline. Plastic 2 mm to 1 m in diameter was collected from the surface within 50 cm range on both sides of the transect line, equating to a 1 m collection width, the entire length of the beach.

As a result of > 50 plastic samples being obtained from all three quadrats, only the common standing-stock beach survey sampling method was used for sampling the following beaches: Pololū Valley, Kaʻaluʻalu Bay, Kaulana Bay, Pine Trees, and Old Kona Airport.

As a result of < 50 plastic samples being obtained using the common standing-stock

beach survey sampling method, the belt transect method was also performed along the high spring-tide/high strandline for the entire length of the beach for the following beaches: North Miloli‘i and South Miloli‘i. On account of sieving difficulties resulting from the damp and compact beach sediment, the belt transect method was also performed for Hilo Bay.

*Rinsing and drying beach plastic samples*

Plastic beach samples were brought back to the lab and rinsed with deionized water. The samples were dried in a convection oven at 45 °C until constant weight, and stored in a desiccator with Drierite prior to sampling with FT-IR (Lares et al. 2018).

*Analyzing beach plastic with FT-IR*

A total of 350 pieces of beach plastic measuring 2 mm to 1 m in diameter were analyzed. Each beach plastic sample was analyzed two times. One spectrum was taken of the sample's surface and the second spectrum was taken of the subsurface, totaling 700 spectra (350 surface and 350 subsurface). The subsurface spectrum was taken by removing $\geq 2$ $mm^2$ area of the plastic sample's surface with a razor blade. Although the subsurface spectrum was analyzed, the subsurface spectrum will be referred to as the inside spectra for the continuation of the manuscript. Each individual spectrum was checked for quality, and the samples were rescanned if peaks were noisy.

Additional metadata was taken from the beach plastic samples. The metadata categories are the following: collection location, presence or absence of outside weathering, presence or absence of fouling, product description, roundness, degradation description, diameter (mm),

color, and plastic polymer class determined by the transmittance bands identification method.

*Preprocessing the beach plastic and standard sample spectra*

The spectra were initially preprocessed by converting all beach plastic and standard sample spectra from percent transmittance values to absorbance units in MATLAB version R2017b. Additional preprocessing techniques were used to process the beach plastic and standard sample spectra for model development. The following techniques were applied in PLS Toolbox 8.6.1 software: Multiplicative Scatter Correction, Second Derivative-Savitzky-Golay, Generalized Least Squares Weighting. The standard sample spectra were preprocessed to help normalize the spectra, eliminate baseline offset, apply derivatives to remove unimportant baseline slope functions, and remove within-class variance while maintaining between-class variance.

*Developing the identification model for class separation*

After preprocessing techniques were applied to the spectra, models were developed and evaluated. The models were built by analyzing five samples of each of the eight plastic polymer standards. The two multivariate classification algorithms of Principal Component Analysis (PCA), an unsupervised machine learning method, and Partial Least Squares Discriminant Analysis (PLS-DA), a supervised machine learning method, were applied separately to the plastic standards to develop the two different models (Hamad et al. 2010; Haware et al. 2011). PCA and PLS-DA algorithm models were tested and the accuracy of each algorithm was assessed in agreement with the following criteria: (1) Separated standards into eight distinct

clusters within the modeled 99% confidence level within a two dimensional space; (2) Created a 99% confidence ellipse around the separated plastic polymer clusters. The models were generated in MATLAB version R2017b and PLS Toolbox 8.6.1 software.

This initial model evaluation addressed hypothesis Ⅰ—testing if the plastic polymer standards could be separated into eight groups according to plastic polymer type through unsupervised machine learning techniques.

*Transmittance bands identification for beach plastics*

Before validating and calibrating unknown beach plastics into the model, the spectra from each of the beach samples were identified based on the presence of predetermined transmittance bands (Tab. 2). Each transmittance band represents a functional group that aids in plastic polymer identification. PET was identified based on the presence of four transmittance bands, PE based on the presence of six transmittance bands, and other beach plastics identified based on the presence of five transmittance bands.

The transmittance bands were selected based on low percent transmittance (pronounced peaks) and chemical structure uniqueness (Corcoran et al. 2009, Jung et al. 2018). Each plastic polymer type has a unique set of peaks, allowing for identification. All predetermined peaks were present for a sample to be classified. Each assigned wavenumber group was accepted within an 11 $cm^{-1}$ range (±5 $cm^{-1}$) of the designated peak wavenumber, to account for slight instrument variations across studies. The surface spectra data were evaluated first. When an identification peak was absent from the surface spectra data, the inside spectra data were then evaluated to determine if all peaks were present. If all peaks were present for the inside spectra

data, the sample was classified according to its inside spectra.

There were seven plastic polymer classes and an unknown class that served as the eight categories for this identification procedure. The classes were the following: PS, ABS, PE, Nylon, PP, PVC, PET, Unknown. Due to the absence in the literature of a reference spectrum for TPE (Thermoplastic elastomer- santoprene-155), TPE was not included in this identification process.

**Table 2.** Plastic Polymer Type, Transmittance Band Identification Peaks, & Chemical Assignment

| **Plastic Polymer Type** | **Transmittance Bands Identification Peaks ($cm^{-1}$)** | **Chemical Assignment (Jung et al. 2018)** |
|---|---|---|
| Polystyrene (PS) | 1. 3024<br>2. 2847<br>3. 1492<br>4. 1451<br>5. 0694 | Aromatic C-H stretch, stretch of aromatic<br>C-H stretch, stretch of methylene<br>Aromatic ring stretch<br>$CH_2$ bend<br>Aromatic CH out-of-plane bend, monosubstituted benzene |
| Acrylonitrile butadiene styrene (ABS) | 1. 2922<br>2. 1494<br>3. 1452<br>4. 0759<br>5. 0698 | C-H stretch<br>Aromatic ring stretch<br>$CH_2$ bend<br>Aromatic CH out-of-plane bend, =CH bend<br>Aromatic CH out-of-plane bend |
| Polyethylene (PE) | 1. 2915<br>2. 2845<br>3. 1472<br>4. 1462<br>5. 0730<br>6. 0717 | C-H stretch of methylene<br>C-H stretch of methylene<br>$CH_2$ bend of methylene<br>$CH_2$ bend of methylene<br>$CH_2$ rock, cis-disubstituted alkene from ethylene monomer<br>$CH_2$ rock, cis-disubstituted alkene from ethylene monomer |
| Nylon 6.6 and nylon 6 (nylon) | 1. 3298<br>2. 2932<br>3. 1634<br>4. 1538<br>5. 0687 | N-H stretch<br>CH stretch<br>C=O stretch<br>NH bend, C-N stretch<br>NH bend, C=O bend |
| Polypropylene (PP) | 1. 2950<br>2. 2915<br>3. 1455<br>4. 1377<br>5. 0840 | C-H stretch<br>C-H stretch of methyl group<br>$CH_2$ bend, deformation of methylene<br>$CH_3$ bend, deformation of methyl<br>$CH_2$ rock, C-$CH_3$ stretch |

| | | |
|---|---|---|
| Polyvinyl chloride (PVC) | 1. 1427<br>2. 1331<br>3. 1255<br>4. 1099<br>5. 0966 | $CH_2$ bend<br>CH bend<br>CH bend<br>C-C stretch<br>$CH_2$ rock |
| Polyethylene terephthalate (PET) | 1. 1713<br>2. 1241<br>3. 1094<br>4. 0720 | C=O stretch of ester<br>C-O stretch of ester<br>C-O stretch<br>Aromatic CH out-of-plane bend, of para-disubstituted benzene |

*Assessing beaches for richness to determine polymer diversity*

After the transmittance band identification for all beach plastic samples was complete, each beach was assessed for species richness. Species richness was determined by the count of plastic polymer types. A richness of four or fewer of the seven plastic polymer categories qualified the beach as having low polymer diversity, thus suggesting that the beach's plastics are ocean-based. A richness of five or more of the seven plastic polymer categories qualified the beach as having high polymer diversity, suggesting that the beach's plastics are ocean-based and land-based. These parameters were determined based on the richness of plastic polymer types found in the Great Pacific Garbage Patch. The four plastic polymer types found in the Great Pacific Garbage Patch were PE, PS, PP, and PVC (Lebreton et al. 2018).

*Exploring the variation between surface and inside spectra*

To explore if there were differences between the surface spectra and inside spectra of the beach plastic samples, both the surface spectra and inside spectra of the plastics found on each of the eight beaches were validated separately by the model. This assessment was determined if there was a discrepancy between the surface spectra and inside spectra samples—giving a greater

understanding of the degradation process and how it is reflected throughout the sample (surface vs. inside). This assessment also evaluated the razor blade method, which was used to obtain the inside spectra. If no significant differences between the surface and inside spectra were found in the results, the razor blade method would be considered redundant and would not be recommended for future studies.

A high discrepancy, especially for the beaches with low polymer diversity, could imply that degradation at the chemical level was taking place on the surface of the beach plastic samples at a different rate than the inside (Satoto et al. 1997, Kiatkamjornwong et al. 1999, Corcoran et al. 2009). This study predicted that degradation would have a greater effect on the surface spectrum making it less likely to fall inside each plastic polymer cluster's 99% confidence ellipse. This discrepancy was thought to be visible in the spectra and validated by the model. If a low discrepancy was observed, especially for the beaches with high polymer diversity, one could infer that little to no degradation at the chemical level was occurring at the surfaces or insides of the beach plastic samples. The study predicted that degradation would affect the inside spectrum less, making the samples more likely to fall inside each plastic polymer cluster's 99% confidence ellipse.

This surface spectra vs. inside spectra assessment addressed hypothesis Ⅱ by evaluating whether the beaches with the highest proportion of ocean-based plastics (low polymer diversity) had plastics with the largest differences between their surface spectra and inside spectra. This hypothesis was evaluated using the following criteria: (1) Each beach's proportion of plastic polymer types based on transmittance band identification was evaluated and plastic polymer diversity was determined. (2) The surface beach samples of each beach were applied to the

model and the number of surface beach samples that fell within each plastic polymer cluster's 99% confidence ellipse were quantified within a two dimensional space. (3) The inside spectra samples of each beach were applied to the model and the number of inside beach samples that fell within each plastic polymer cluster's 99% confidence ellipse were quantified within a two dimensional space. This assessment planned to give greater insight into the stages of degradation of the spectra before they are calibrated into the model.

*Exploring degradation*

To determine if there was a relationship between the presence of visible outside weathering (yellow or white discoloration on the surface) on the beach plastic samples and photodegradation seen in the surface spectra samples, the carbonyl index method was explored (Andrady et al. 1993, Kiatkamjornwong et al. 1999, Endo et al. 2005, Fotopoulou and Karapanagioti 2012, Yousif and Haddad 2013). The index was developed to identify the intensity of a carbonyl functional group within the FT-IR spectrum. The carbonyl functional group develops within a specific wavenumber range when the plastic polymer experiences light-induced photooxidation, which is photodegradation in the presence of air (Satoto et al. 1997, Kiatkamjornwong et al. 1999). This relationship was explored by calculating a carbonyl index for PE and PS. Polyethylene was selected because it is the world's most produced plastic polymer (Geyer et al. 2017), Polyethylene is the most abundant plastic polymer identified in FT-IR studies, and PE was predicted to be sampled at all eight beaches. Polystyrene was also evaluated because it is more susceptible to outdoor weathering than other plastic polymers and has the potential to serve as a land-based source indicator (Gewert et al. 2015).

*Calculating the carbonyl index (CI)*

The carbonyl index (CI) is on a 0 to >1 scale. A value of 1 or greater indicates a strong carbonyl peak, demonstrating that the plastic polymer has been significantly transformed (Syakti et al. 2017). First, the CI was calculated by converting the FT-IR spectrum from percent transmittance to percent absorbance.

The CI for PE was calculated by taking the percent absorbance at 1717 (±2) $cm^{-1}$; the location of the carbonyl peak, and dividing the percent absorbance at 720 (±2) $cm^{-1}$; a reference peak region. (Andrady et al. 1993, Satoto et al. 1997, Endo et al. 2005, Fotopoulou and Karapanagioti 2012).

**Carbonyl Index PE = A1717 $cm^{-1}$ /A720 $cm^{-1}$**

- A1717 $cm^{-1}$ = Absorbance of the carbonyl group (C=O)
- A720 $cm^{-1}$ = Absorbance of the $CH_2$ rock, cis-disubstituted alkene from ethylene monomer

The CI for PS was calculated by taking the percent absorbance at 1743 (±2) $cm^{-1}$; the location of the carbonyl peak, and dividing the percent absorbance at 1451 (±2) $cm^{-1}$; a reference peak region (Kiatkamjornwong et al. 1999, Yousif and Haddad 2013).

**Carbonyl Index PS = A1743 $cm^{-1}$ /A1451 $cm^{-1}$**

- A1743 $cm^{-1}$ = Absorbance of the carbonyl group (C=O)
- A1451 $cm^{-1}$ = Absorbance of the internal standard band, in the PS backbone chain

Carbonyl index varies among plastic polymers and among studies, and no specific index number is standardized to represent full carbonyl peak development. Therefore, additional categorical statistics were performed and carbonyl peaks were marked present if the sample's carbonyl index was greater than the mean carbonyl indices of the PE and PS plastic polymer standards. The PE and PS plastic polymer standards were sourced from recycling bins and were absent of outside weathering. The proportion of plastic polymers (PE and PS) marked present for outside weathering per beach were recorded as well as the separate CI indices for each polymer type. This procedure permitted the observation of multivariable degradation trends and fewer assumption limitations.

This analysis addressed hypothesis Ⅲ by evaluating if there was a significant correlation between the presence of outside weathering and the presence of a carbonyl peak within the surface spectra of the PE and PS beach samples. This hypothesis Ⅲ was evaluated by using the following criteria: (1) Outside weathering was marked as present or absent for all PE and PS beach samples. (2) Carbonyl peaks were marked present if the sample's carbonyl index was greater than the mean carbonyl index of the PE and PS standards.

(3) The predetermined carbonyl group wavenumber regions were evaluated for all 40 surface PS samples and 86 surface PE samples.

The goal of this assessment was to develop a deeper understanding of the relationship between the physical and the chemical weathering of beach plastic polymers.

*Calibrating beach plastic samples into the standard model*

Beach plastic samples were calibrated into the final standard model, which was built from 96 identified plastic polymer standards (12 spectra standards for each of the eight polymer types). The calibrated models were assessed in agreement with the following criteria: (1) Separated plastic polymer classes into eight distinct clusters, with the beach plastics incorporated in the model's original framework, within the modeled 99% confidence limit within a two dimensional space; (2) Created a 99% confidence ellipse around the separated plastic polymer clusters within a two dimensional space. The calibrated models were generated in MATLAB version R2017b and PLS Toolbox 8.6.1 software.

*Testing the classification tool*

The accuracy of the final FT-IR classification tool was assessed by determining the percentage of beach plastic samples that were classified by the model. The beach plastic samples were classified according to the following criteria: (1) If the validated beach plastic sample fell within a plastic polymer cluster's 99% confidence ellipse and was identified as that plastic polymer type according to its transmittance band identification, the sample was marked as identified by the model. (2) If the beach plastic sample fell within a plastic polymer cluster's 99% confidence ellipse and was identified as an unknown plastic polymer type according to its transmittance band identification, the sample was marked as identified by the model.

## Results

*Hypothesis* Ⅰ

Two models were built to address hypothesis Ⅰ to test if the plastic polymer standards could be separated into eight groups according to plastic polymer type through machine learning techniques. The two multivariate classification algorithms of Principal Component Analysis (PCA), an unsupervised machine learning method, and Partial Least Squares Discriminant Analysis (PLS-DA), a supervised machine learning method were used to build the models. PCA and PLS-DA classification algorithms were applied to the plastic polymer standards and assessed in agreement with the following criteria: (1) Separated standards into eight distinct clusters within the modeled 99% confidence limit within a two or three dimensional space; (2) Created a 99% confidence ellipse around the separated plastic polymer clusters.

*Model building and preprocessing*

The model was developed using MATLAB version R2017b and PLS Toolbox 8.6.1 software. Spectra were produced with a Shimadzu IRAffinity-1 FT-IR instrument using the attenuated total reflectance (ATR) method, and generated spectra from the wavenumber range of 650 $cm^{-1}$ to 4000 $cm^{-1}$. The model foundation was built by analyzing 12 spectra samples of each of the eight plastic polymer standards. Preprocessing techniques were applied to all 96 plastic polymer standard spectra before the model was generated. Each spectrum had a total of 1739 variables.

The preprocessing techniques applied to the spectra were the following: transmission to absorbance (log(1/T)), multiplicative scatter correction, Savitzky-Golay; second derivative with

a third polynomial order, generalized least squares weighting, and mean centering. Preprocessing techniques were used to normalize the spectra, eliminate baseline offset, apply derivatives to remove unimportant signals and remove within-class variance while maintaining between-class variance. Polystyrene (PS) and acrylonitrile butadiene styrene (ABS) could not be separated without the application of the preprocessing techniques mentioned above.

*Model building algorithms and confidence limits*

The two multivariate classification algorithms of Principal Component Analysis (PCA) and Partial Least Squares Discriminant Analysis (PLS-DA) were applied separately to the model foundation. The confidence ellipses around each plastic polymer standard class in both the PCA and PLS-DA models were generated using Hotelling's T-squared statistic and the overall confidence limit was calculated by applying the Student's t-distribution (Wise et al. 1990). The overall confidence limit for both models and their confidence ellipse limits that outlined each class was set to 99%. This decision was based on the known identity of the plastic polymer standards and the calibration goals of the model. Setting the confidence limit to 99% increased the model's confidence ellipse, which resulted in the inclusion of more samples.

*Model building scores and separation*

The PCA Plastic Polymer Standard Model (Fig. 1) was generated with six principal components, built with the first two principal components, and separated the data while meeting all evaluation criteria requirements. The first two principal component scores captured 53.92% of the variance in the data set (Tab. 3). The PLS-DA Plastic Polymer Standard Model (Fig. 2) was

generated with six latent variables, built with the first two latent variables, and separated the data based on the criteria. The first two latent variable scores captured 53.92% of the variance in the data set (Tab. 4), which was the same as the PCA model.

For both the PCA and PLS-DA models the known plastic polymer standard classes were separated into colored clusters. Each of the colored clusters represented one of the following eight plastic polymer standard types: polyethylene terephthalate (PET), polyethylene (PE), polyvinyl chloride (PVC), polypropylene (PP), polystyrene (PS), nylon (nylon), acrylonitrile butadiene styrene (ABS), and thermoplastic elastomer (TPE).

The score and latent variable plots display the relationship between plastic polymer types. PET, in the lower left quadrant for PCA (Fig. 1) and the upper left quadrant for PLS-DA (Fig. 2), appeared as the most unique plastic polymer spectra in the model for this data set. The distance between PET and any of the other seven plastic polymer standards was further than the distance between any of the seven plastic polymer spectra groups in both model plots. PET contains an ester functional group that is absent from the other seven plastic polymer standards. Three out of four predetermined transmittance bands for PET, that served as identification peaks, are unique to the PET chemical structure and are also absent in the other plastic polymer standards. The scores and distances between polymer spectra classes trends are consistent across both models. The scores assume that polymer spectra with similar scores are similar.

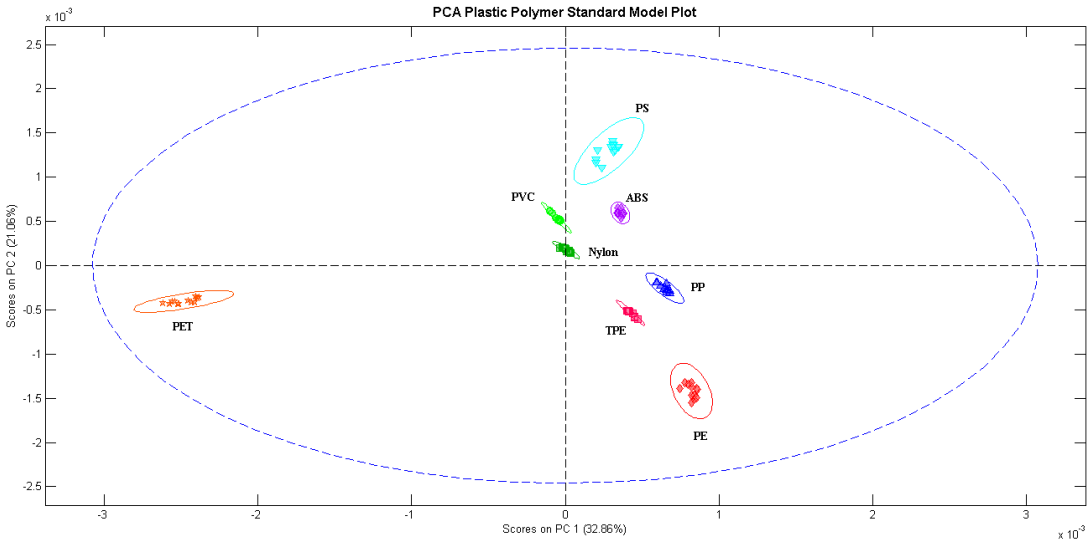


**Figure 1.** PCA Plastic Polymer Standard Model built by analyzing 96 plastic polymer standard spectra. The figure shows Principal Component (PC) Scores 1 plotted against Principal Component (PC) Scores 2. Each colored cluster represents one of the known plastic polymer standard classes. The following are the 8 plastic polymer standard classes represented above: polyethylene terephthalate (PET), polyethylene (PE), polyvinyl chloride (PVC), polypropylene (PP), polystyrene (PS), nylon (nylon), acrylonitrile butadiene styrene (ABS), and thermoplastic elastomer (TPE). Prepared in MATLAB version R2017b software and PLS Toolbox 8.6.1 software.

**Table 3.** Percent Variance Captured by PCA Model

| Principal Component Number | Eigenvalue of Covariance (X) | % Variance Captured this PC | % Variance Captured Total |
|---|---|---|---|
| 1 | 9.68e-07 | 32.86 | 32.86 |
| 2 | 6.20e-07 | 21.06 | 53.92 |
| 3 | 4.71e-07 | 16.01 | 69.93 |
| 4 | 4.05e-07 | 13.75 | 83.67 |
| 5 | 2.69e-07 | 9.14 | 92.82 |
| 6 | 1.33e-07 | 4.53 | 97.35 |

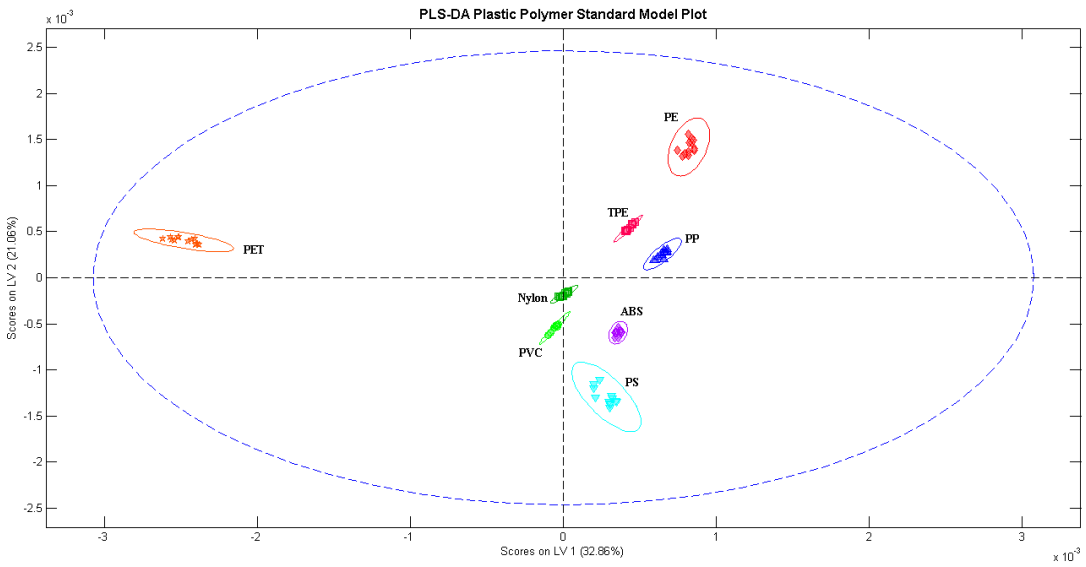


**Figure 2.** PLS-DA Plastic Polymer Standard Model built by analyzing 96 plastic polymer standard spectra. The figure shows Latent Variable (LV) Scores 1 plotted against Latent Variable (LV) Scores 2. Each colored cluster represents one of the known plastic polymer standard classes. The following are the eight plastic polymer standard classes represented above: polyethylene terephthalate (PET), polyethylene (PE), polyvinyl chloride (PVC), polypropylene (PP), polystyrene (PS), nylon (nylon), acrylonitrile butadiene styrene (ABS), and thermoplastic elastomer (TPE). Prepared in MATLAB version R2017b software and PLS Toolbox 8.6.1 software.

**Table 4.** Percent Variance Captured by PLS-DA Model

| | X-Block | | Y-Block | |
|---|---|---|---|---|
| Latent Variable | This | Total | This | Total |
| 1 | 32.86 | 32.86 | 14.26 | 14.26 |
| 2 | 21.06 | 53.92 | 14.23 | 28.49 |
| 3 | 16.01 | 69.93 | 14.24 | 42.73 |
| 4 | 13.75 | 83.67 | 14.22 | 56.95 |
| 5 | 9.14 | 92.82 | 14.18 | 71.13 |
| 6 | 4.53 | 97.35 | 14.13 | 85.25 |

*Plastic polymer standard model results*

With identical inputs and preprocessing of the spectra samples, the PCA and PLS-DA algorithms were nearly identical in modeling the separation of the eight plastic polymer standards classes. Both the PCA and PLS-DA Plastic Polymer Standard Models met the elevation criteria; however, PCA Plastic Polymer Standard Model served as the only unsupervised machine learning method.

The PCA Plastic Polymer Standard Model was selected as the tool to continue research development. This decision was made as a result of the PCA algorithm's unsupervised learning ability to detect data anomalies and outliers. The ability of PCA to detect anomalies and learn by itself was thought to be advantageous when calibrating beach plastics into the model. Beach plastics not only have the potential of being a heterogeneous mixture of plastic polymer types, but can also exhibit chemical degradation signals as a result of outside weathering effects.

Although the PLS-DA Plastic Polymer Standard Model has its advantages and is recommended for further investigation in future studies, the PCA algorithm provided a statistically robust model to test hypothesis Ⅱ and lay the framework for the final plastic identification tool.

*Hypothesis* Ⅱ

The beaches with the highest proportion of ocean-based plastics (low polymer diversity) will have plastics with the largest differences between their surface spectra and their inside spectra. This was tested by (1) Determining the plastic polymer types of the the beach plastic samples with the transmittance band method; (2) Determining each of the eight beaches plastic

diversity; (3) Applying both the surface and inside beach spectra to the PCA Plastic Polymer Standard Model and quantifying whether the sample spectra fell within one of the eight plastic polymer standard classes' confidence ellipses; (4) Calculating the proportional differences between inside and surface beach sample spectra identified with the PCA Plastic Polymer Standard Model.

*Beach plastic transmittance bands identification results*

To validate the beach plastic samples before the samples were calibrated into the model, The plastic polymer types of all beach plastics were identified with the transmittance bands identification method (Tab. 5). This identification was based on the presence of predetermined transmittance bands. Seven plastic polymer types were identified from the beach plastic samples from the eight beach locations. Out of the 350 beach plastic samples evaluated, 17 beach plastic samples were identified as not fitting the criteria for any of the seven plastic polymer types and placed in the Unknown category.

**Table 5.** Plastic Polymer Types and Counts by Beach

| **Plastic Type** | *Kaulana Bay* | *Hilo Bay* | *Ka'alu'alu Bay* | *Kona Airport* | *North Miloli'i* | *South Miloli'i* | *Pololū Valley* | *Pine Trees* |
|---|---|---|---|---|---|---|---|---|
| PE | 30 | 20 | 35 | 32 | 4 | 13 | 26 | 44 |
| PP | 18 | 8 | 14 | 16 | 9 | 4 | 19 | 4 |
| PS | 0 | 13 | 0 | 1 | 8 | 0 | 5 | 1 |
| PET | 0 | 3 | 0 | 0 | 0 | 0 | 0 | 0 |
| Nylon | 0 | 2 | 0 | 0 | 3 | 0 | 0 | 0 |
| PVC | 0 | 0 | 0 | 0 | 0 | 0 | 0 | 0 |

| | | | | | | | | |
|---|---|---|---|---|---|---|---|---|
| ABS | 0 | 0 | 0 | 0 | 1 | 0 | 0 | 0 |
| Unknown | 2 | 4 | 1 | 1 | 8 | 0 | 0 | 1 |

*Plastic polymer diversity results*

Polymer diversity for each of the eight beaches was determined. Six beaches had a low polymer diversity of < 4 plastic polymer types (Tab. 6). Kaulana Bay had a total of three types, Ka'alu'alu Bay had a total of three types, Kona Airport had a total of three types, South Miloli'i had a total of two types, Pololū Valley had at total of three types, and Pine Trees had a total of four types. North Miloli‘i and Hilo Bay were the two beaches that had a high polymer diversity of > 4 plastic polymer types (Tab. 7). Hilo Bay had a total of six types and North Miloli'i had a total of six types out of the eight plastic polymer categories.

**Table 6.** Low Plastic Polymer Diversity Beaches and Quantity of Plastic Types

| **Kaulana Bay** | **Ka'alu'alu Bay** | **Kona Airport** | **South Miloli'i** | **Pololū Valley** | **Pine Trees** |
|---|---|---|---|---|---|
| 3 | 3 | 3 | 2 | 3 | 4 |

**Table 7.** High Plastic Polymer Diversity Beaches and Quantity of Plastic Types

| **Hilo Bay** | **North Miloli'i** |
|---|---|
| 6 | 6 |

*Surface and inside spectra identified by the plastic polymer standard spectra model*

To determine if there was a detectable difference between the beach plastic samples' surface and inside spectra, both were applied separately to the PCA Plastic Polymer Standard Model. The surface and inside spectra were evaluated and quantified whether the spectra fell within one of the eight plastic polymer standard classes' confidence ellipses. The results of the model identification were organized by beach and were cross validated with the identification of the Transmittance Band Method (Tab. 8). For Kaulana Bay, Hilo Bay, Ka'alu'alu Bay, Kona Airport, South Miloli'i, Pololū Valley, and Pine Trees inside spectra identification was greater than surface spectra identification of beach plastics when applied to the model. North Miloli'i was the only beach where surface spectra identification of beach plastics was greater than inside spectra identification (Fig. 3).

**Table 8.** PCA Plastic Polymer Standard Spectra Model Identification Count Results by Beach

| Beach | Surface | Inside | Total Identified Samples by Transmittance Bands |
|---|---|---|---|
| Kaulana Bay | 6 | 15 | 48 |
| Hilo Bay | 12 | 18 | 46 |
| Ka'alu'alu Bay | 6 | 16 | 49 |
| Kona Airport | 12 | 24 | 50 |
| North Miloli'i | 11 | 8 | 25 |
| South Miloli'i | 1 | 4 | 17 |
| Pololū Valley | 8 | 24 | 50 |
| Pine Trees | 10 | 19 | 49 |

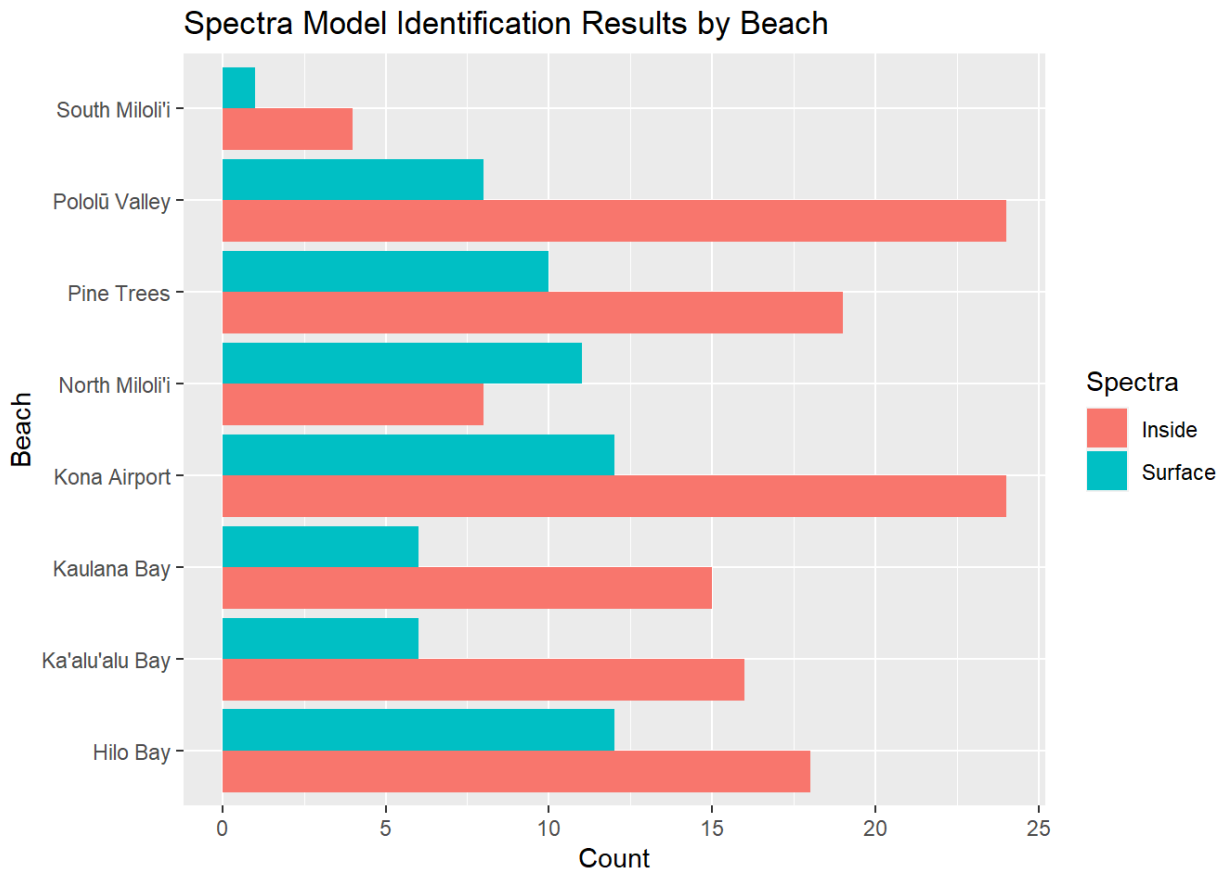


**Figure 3.** Quantifies the number of the beach samples' plastic polymer types that were identified by the PCA model. The surface totals represent the surface spectra that fell within each plastic polymer cluster's 99% confidence ellipse. The inside totals represent the inside spectra that fell within each plastic polymer cluster's 99% confidence ellipse.

*Statistical analysis of proportional differences*

To determine the proportional differences between surface and inside plastic polymer spectra identified with the PCA Plastic Polymer Standard Model, a 2-sample test for equality of proportions without continuity correction with a two-sided alternative hypothesis was used in R version 3.5.3 software.

The following low polymer diversity beaches, Kaulana Bay (X-squared = 4.937, df = 1, n = 48, p-value = 0.026), Ka'alu'alu Bay (X-squared = 5.861, df = 1, n = 49, p-value = 0.015),

Kona Airport (X-squared = 6.25, df = 1, n = 50, p-value = 0.012), types), Pololū Valley (X-squared = 11.765, df = 1, n = 50, p-value = < 0.001), and Pine Trees (X-squared = 3.967, df = 1, n = 49, p-value = 0.046) had significant differences between the surface and inside spectra classification.

The beaches that had a high polymer diversity, Hilo Bay (X-squared = 1.780, df = 1, n = 46, p-value = 0.182) and North Miloli'i (X-squared = 0.764, n = 25, df = 1, p-value = 0.382) did not have significant differences between their surface and inside spectra classifications.

South Miloli'i (X-squared = 2.11, df = 1, n = 17, p-value = 0.146) had low polymer diversity and did not have significant differences between its surface and inside spectra classifications. This result may be attributed to its low sample size (n = 17). Both South Miloli'i (n = 17) and North Miloli'i (n = 25) had lower sample sizes of identified spectra than the other six beaches.

When combining all six low polymer diversity beaches there was a significant difference between the model identification of the surface and inside spectra (2-sample test for equality of proportions without continuity correction with a two-sided alternative hypothesis: X-squared = 33.143, df = 1, n = 263, p-value= < 0.001).

When combining the two high polymer diversity beaches there was no significant detectable difference between the model identification of the surface and inside spectra beach samples (2-sample test for equality of proportions without continuity correction with a two-sided alternative hypothesis: X-squared = 0.281, df = 1, n = 71, p-value = 0.5964).

When examining all eight beaches together there was a significant difference between the model identification of the surface and inside spectra beach samples (2-sample test for equality

of proportions without continuity correction with a two-sided alternative hypothesis: X-squared = 27.924, df = 1, n = 71,  p-value = < 0.001).

**Table 9.** Spectra Model Identification Count Results for All Beaches Combined

| Surface | Inside | Total Identified Samples by Transmittance Bands |
|---|---|---|
| 66 | 128 | 334 |

*Beach polymer proportion results*

There was a detectable significant difference between the surface and inside beach spectra from beaches with a low polymer diversity, by the PCA Plastic Polymer Standard Model. These results indicate that degradation at the chemical level occurred on the surface of the beach plastic samples, at a different rate, than the inside of the beach plastics sampled. For all beaches, besides North Miloli'i, inside spectra identification (n = 128) was greater than surface spectra identification (n = 66)  by the PCA Plastic Polymer Standard Spectra Model. Based on these results, the razor blade method, used to analyze the inside spectra of the plastic sample, is recommended for future plastic identification studies, especially for beaches with low plastic polymer diversity.

*Hypothesis* Ⅲ

There will be a significant correlation between the presence of outside weathering and the presence of a carbonyl peak within the surface spectra of polyethylene (PE) and polystyrene (PS) beach samples.

*Presence of outside weathering*

Outside weathering was marked as present or absent for all polyethylene (PE) and polystyrene (PS) beach samples. A sample was marked present for outside weathering if the surface of the sample had visible yellow or white discoloration.

**Figure 4.** Outside weathering was marked as present or absent for all polyethylene (PE) and polystyrene (PS) beach samples. The images above are examples of samples that were marked present for outside weathering. A sample was marked present for outside weathering if the surface of the plastic sample had visible yellow or white discoloration.

PE was present at all eight beaches sampled. A total of 204 samples of PE were verified by the transmittance band method. Out of the 204 samples of PE, 74 samples were assessed for

outside weathering. Ten samples of PE were assessed from seven of the eight beaches. Four samples of PE were assessed from North Miloli'i. Of the 74 PE samples, outside weathering was marked present for 43 samples and absent for 31 samples.

PS was present at five of the eight beaches sampled. A total of 28 samples of PS were verified by the transmittance band method. Out of the 28 samples of PS, all 28 samples were assessed for outside weathering. Of the 28 PE samples, outside weathering was marked present for 21 samples and absent for seven samples.

**Table 10.** Presence of Outside Weathering

| **Plastic Polymer Type** | **Beach Samples Assessed** | **Weathering Present** | **Weathering Absent** |
|---|---|---|---|
| Polyethylene (PE) | 74 | 43 | 31 |
| Polystyrene (PS) | 28 | 21 | 7 |

*Average carbonyl index for PE & PS standards*

The carbonyl peaks of the spectra were assessed in absorbance mode. Carbonyl peaks were marked present if the sample's carbonyl index (CI) was greater than the mean carbonyl index of the PE and PS standards. The carbonyl index (CI) was on a 0 to >1 scale. A value of 1 or greater indicates a strong carbonyl peak. The average carbonyl index for the 12 PE standard spectra that were used to develop the identification model was 0.074. The average carbonyl index for the 12 PS standard spectra that were used to develop the model was 0.223. The PS standards mean carbonyl index was greater than the PE standards mean carbonyl index.

*Carbonyl index for PE and PS beach samples*

For the 74 beach samples of PE that were assessed, the average carbonyl index (CI) was 0.229. For the 28 beach samples of PS that were assessed, the average carbonyl index (CI) was 0.397.

**Table 11.** Carbonyl Index for PE and PS Samples

| **Plastic Polymer Type** | **Standard (CI) Average** | **Beach Sample (CI) Average** |
|---|---|---|
| Polyethylene (PE) | 0.074 | 0.229 |
| Polystyrene (PS) | 0.223 | 0.397 |

*Presence of Outside Weathering & the Presence of a Carbonyl Peak for Polyethylene (PE)*

$H_0$: Assumes that there is no relationship between the presence of outside weathering and the presence of a carbonyl peak within polyethylene (PE) beach samples.

$H_1$: Assumes that there is a relationship between the presence of outside weathering and the presence of a carbonyl peak within polyethylene (PE) beach samples.

*Pearson's Chi-squared test for PE*

Pearson's Chi-squared test with Monte Carlo simulation was performed in R version 3.5.3 software to determine the relationship between presence of outside weathering and the presence of a carbonyl peak for polyethylene (PE). No significant relationship was detected (Pearson's Chi-squared test with Monte Carlo simulation: x-squared = 0.094, df= 1, p-value = 1), resulting in a failure to reject the null hypothesis as there is no observed relationship between the presence

of outside weathering and the presence of a carbonyl peak within the surface spectra of the PE beach samples.

*Fisher's exact test for count data for PE*

As a result of a small data set and high frequency of small cell counts, a Fisher's Exact Test for Count Data with a two-sided alternative was performed in R version 3.5.3 software to determine the relationship between presence of outside weathering and the presence of a carbonyl peak for polyethylene (PE).

No significant relationship was detected (Fisher's Exact Test for Count Data: n= 74, odds ratio = 0.687, p-value = 1), resulting in a failure to reject the null hypothesis due to no evidence that the presence of outside weathering signifies a presence of a carbonyl peak within the surface spectra of PE beach samples. The low odds ratio indicates an insignificant inverse relationship between the two groups.

**Table 12.** Presence of Outside Weathering & Carbonyl Peak for PE

| Polyethylene (PE) | **Carbonyl Peak** | |
|---|---|---|
| **Outside Weathering** | Absent | Present |
| Absent | 1 | 30 |
| Present | 2 | 41 |

*Presence of outside weathering & the presence of a carbonyl peak for polystyrene (PS)*

$H_0$: Assumes that there is no relationship between the presence of outside weathering and

the presence of a carbonyl peak within polystyrene (PS) beach samples.

$H_1$: Assumes that there is a relationship between the presence of outside weathering and the presence of a carbonyl peak within polystyrene (PS) beach samples.

*Pearson's Chi-squared test for PS*

Pearson's Chi-squared test with Monte Carlo simulation was performed in R version 3.5.3 software to determine the relationship between presence of outside weathering and the presence of a carbonyl peak for polystyrene (PS). A significant relationship was detected (Pearson's Chi-squared test with Monte Carlo simulation: x-squared = 6.462, df= 1, p-value = 0.049), supporting the alternative hypothesis and assuming there is an observed relationship between the presence of outside weathering and the presence of a carbonyl peak within the surface spectra of the PS beach samples.

*Fisher's exact test for count data for PS*

As a result of a small data set and high frequency of small cell counts, a Fisher's Exact Test for Count Data with a two-sided alternative was performed in R version 3.5.3 software to determine the relationship between presence of outside weathering and the presence of a carbonyl peak for polystyrene (PS).

No significant relationship was detected (Fisher's Exact Test for Count Data: n= 28, odds ratio = infinity, p-value = 0.056), resulting in a failure to reject the null hypothesis due to no evidence that the presence of outside weathering signifies a presence of a carbonyl peak within

the surface spectra of PS beach samples. The high odds ratio indicates an insignificant direct relationship between the two groups.

**Table 13.** Presence of Outside Weathering & Carbonyl Peak for PS

| Polystyrene (PS) | **Carbonyl Peak** | |
|---|---|---|
| **Outside Weathering** | Absent | Present |
| Absent | 2 | 5 |
| Present | 0 | 21 |

*Results of outside weathering & presence of CI peak for PE & PS beach samples*

The presence of outside weathering does not serve as a significant indicator of the presence of a carbonyl peak within the surface spectra of polyethylene (PE) and polystyrene (PS) beach samples. Considering the low p-value, high odds ratio, and small sample size, more data are needed to determine if the presence of outside weathering can be a significant indicator for the presence of carbonyl peaks for polystyrene beach samples. To further understand the relationship, a more detailed exploration of carbonyl peaks and their carbonyl indices within the different plastic polymer groups was taken.

*Carbonyl peaks & carbonyl indices evaluated*

To further investigate the relationship between outside weathering and carbonyl peaks of beach plastics, the carbonyl indices for the polyethylene (PE) and polystyrene (PS) standards were evaluated. The mean carbonyl indices for the polyethylene (PE) and polystyrene (PS) standards were then compared to the mean carbonyl indices of the degraded and non-degraded

beach samples. Beach samples were marked as degraded if the surface of the sample had visible yellow or white discoloration. Beach samples were marked as non-degraded if the surface of the sample did not have visible yellow or white discoloration.

*PE standard (CI) & PE degraded sample (CI)*

| **Polyethylene (PE) Sample Group** | **Carbonyl Index(CI) Mean** | **Standard Deviation** |
|---|---|---|
| PE Standard | 0.074 | 0.0285 |
| PE Degraded | 0.245 | 0.1426 |

*T-Test & Power Calculation PE Standard (CI) & PE Degraded Sample (CI)*

$H_0$: The carbonyl index (CI) mean for the PE Degraded sample and PE Standard groups are equal. This assumes that there is no detectable difference between the mean carbonyl peak of the PE Standard (CI) and PE Degraded Sample (CI) groups; both PE groups have experienced equal chemical degradation.

$H_1$: The PE Degraded Sample group has a greater mean carbonyl index (CI) than the PE Standard group. This assumes the PE Degraded Sample (CI) group is more chemically degraded than the PE Standard (CI) group.

Welch's two sample t-test using the alternative greater argument was performed in R version 3.5.3 software to determine the difference in the means of carbonyl index peaks for the Degraded Sample (CI) and Standard (CI) polyethylene (PE) groups. A significant relationship was detected (Welch's two sample t-test alternative greater: $t = 7.375$, $df = 50.912$, PE Degraded

Sample (CI) sd = 0.1426, PE Standard (CI) sd = 0.0285, p= <0.001 ), supporting the alternative hypothesis and assuming the PE Degraded Sample (CI) group is more chemically degraded than the PE Standard (CI) group.

A two-sample t-test power calculation with unequal sample sizes and unequal variances was also performed (PE Degraded Sample (CI) n = 43, PE Standard (CI) n= 12, delta = 0.172, sig.level = 0.05, alternative = one.sided, power = 1). This calculation resulted in a high power value, supporting that there was a reliable difference detected between the group means.

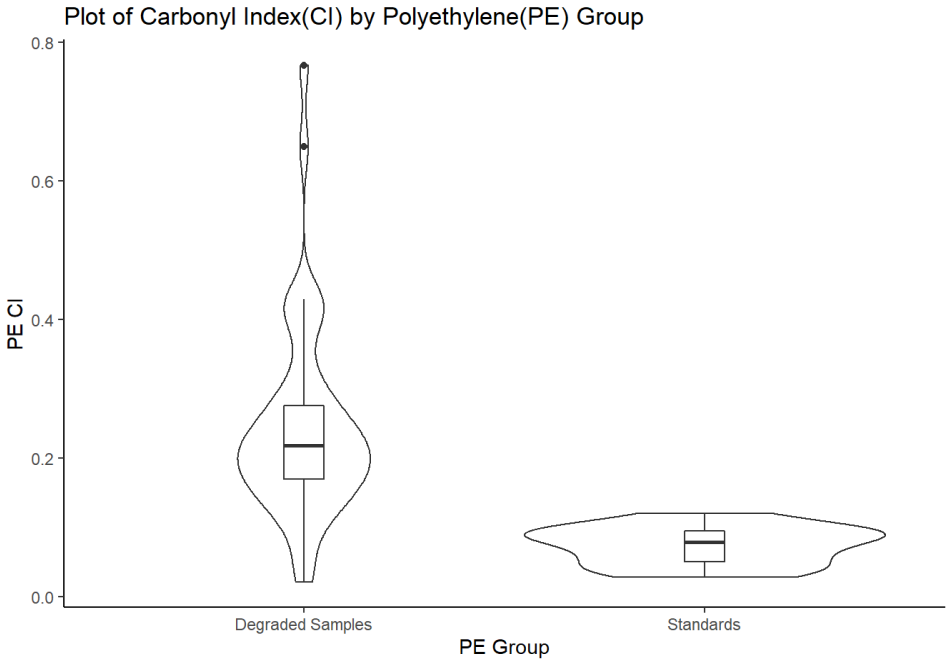


**Figure 5.** Violin plot of carbonyl index (CI) for PE standards and PE degraded samples.

*PE standard (CI) & PE non-degraded sample (CI)*

| **Polyethylene (PE) Sample Group** | **Carbonyl Index(CI) Mean** | **Standard Deviation** |
|---|---|---|
| PE Standard | 0.074 | 0.0285 |
| PE Non-Degraded | 0.207 | 0.0989 |

*T-Test & power calculation PE standard (CI) & PE non-degraded sample (CI)*

$H_0$: The carbonyl index mean for the PE Non-Degraded sample and PE Standard groups are equal. This assumes that there is no detectable difference between the mean carbonyl peak of the PE Standard (CI) and PE Non-Degraded Sample (CI) groups; both PE groups have experienced equal chemical degradation.

$H_1$: The PE Non-Degraded Sample group has a greater mean carbonyl index than the PE Standard group. This assumes the PE Non-Degraded Sample (CI) group is more chemically degraded than the PE Standard (CI) group.

Welch's two sample t-test using the alternative greater argument was performed in R version 3.5.3 software to determine the difference in the means of carbonyl index peaks for the Non-Degraded Sample (CI) and Standard (CI) polyethylene (PE) groups. A significant relationship was detected (Welch Two Sample t-test alternative greater: t = 6.7912, df = 39.327, PE Non-Degraded Sample (CI) sd= 0.0989 , PE Standard (CI) sd = 0.0285, p= <0.001 ), supporting the alternative hypothesis and assuming the PE Non-Degraded Sample (CI) group is more chemically degraded than the PE Standard (CI) group.

A two-sample t-test power calculation with unequal sample sizes and unequal variances was also performed (PE Non-Degraded Sample (CI) n = 31, PE Standard (CI) n= 12, delta = 0.133, sig.level = 0.05, alternative = one.sided, power = 0.9999998 ). This calculation resulted in a high power value supporting that there was a reliable difference detected between the group means.

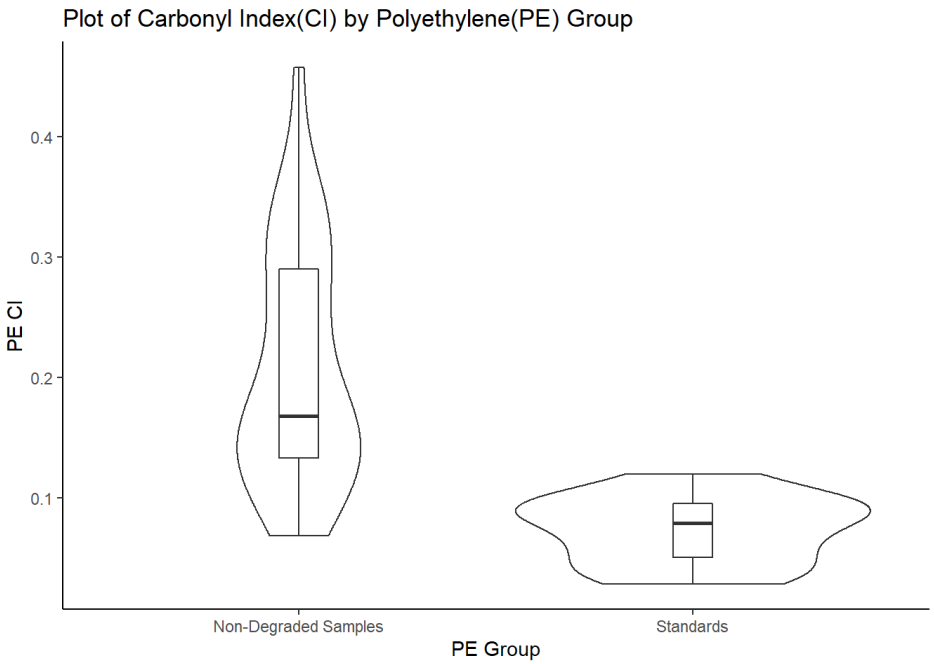


**Figure 6.** Violin plot of carbonyl index (CI) for PE standards and PE non-degraded samples.

*PE non-degraded (CI) & PE degraded sample (CI)*

| **Polyethylene (PE) Sample Group** | **Carbonyl Index(CI) Mean** | **Standard Deviation** |
|---|---|---|
| PE Non-Degraded | 0.207 | 0.0989 |
| PE Degraded | 0.245 | 0.1426 |

*T-Test & power calculation PE non-degraded (CI) & PE degraded sample (CI)*

$H_0$: The carbonyl index mean for the PE Degraded sample and PE Non-Degraded sample groups are equal. This assumes that there is no detectable difference between the mean carbonyl peak of the PE Degraded Sample (CI) and PE Non-Degraded Sample (CI) groups; both PE groups have experienced equal chemical degradation.

$H_1$: The PE Degraded Sample group has a greater mean carbonyl index than the PE Non-Degraded Sample group. This assumes the PE Degraded Sample (CI) group is more chemically degraded than the PE Non-Degraded Sample (CI) group.

Welch's two sample t-test using the alternative greater argument was performed in R version 3.5.3 software to determine the difference in the means of carbonyl index peaks for the Degraded Sample (CI) and Non-Degraded Sample (CI) polyethylene (PE) groups. No significant relationship was detected (Welch's two sample t-test alternative greater: t = 1.3724, df = 71.92, PE Degraded Sample (CI) sd= 0.1426, PE Non-Degraded Sample (CI) sd= 0.0989, p= 0.087 ), resulting in a failure to reject the null hypothesis due to no evidence that the PE Degraded Sample (CI) group is more chemically degraded than the PE Non-Degraded Sample (CI) group.

A two-sample t-test power calculation with unequal sample sizes and unequal variances was also performed (PE Degraded (CI) n = 43, PE Non-Degraded Sample (CI) n = 31, delta = 0.039, sig.level = 0.05, alternative = one.sided, power = 0.388 ). This calculation resulted in a low power value supporting that the small sample size limits the detection of a reliable difference between the group means.

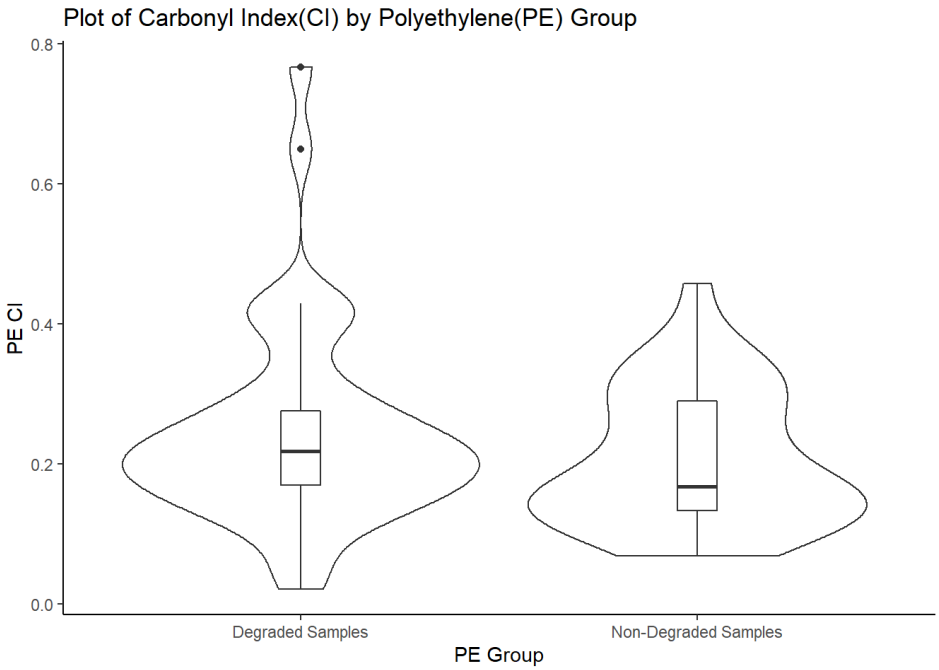


**Figure 7.** Violin plot of carbonyl index (CI) for PE degraded and PE non-degraded samples.

*PE standard (CI), PE non-degraded (CI), & PE degraded sample (CI) mean plots*

| **PE Standard (CI) Average** | **PE Non-Degraded Sample (CI) Average** | **PE Degraded Sample (CI) Average** |
|---|---|---|
| 0.074 | 0.207 | 0.245 |

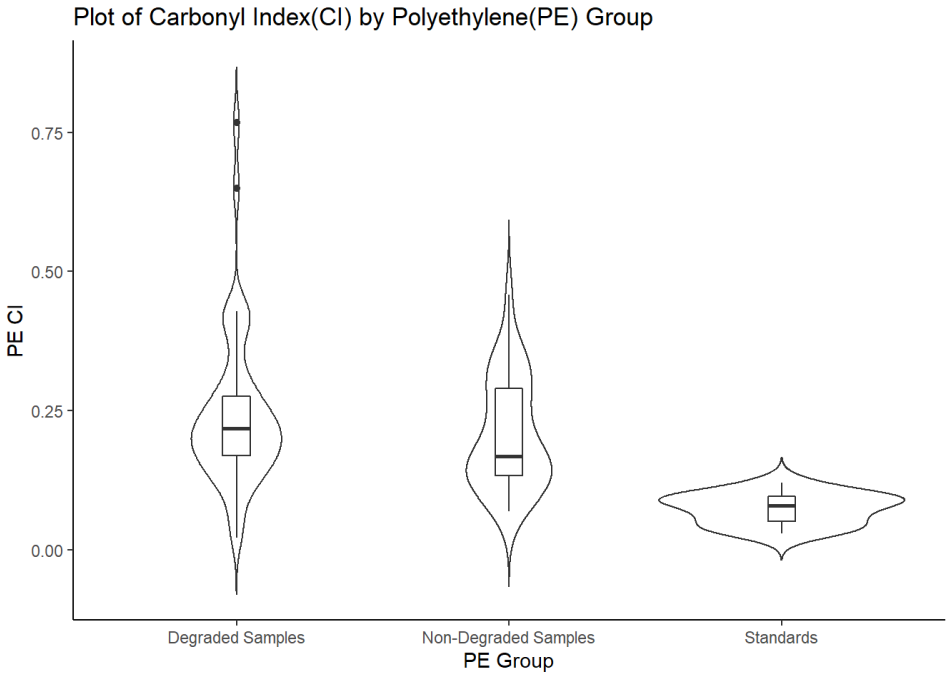


**Figure 8.** Violin plot of carbonyl index (CI) for PE standards, PE non-degraded samples, and PE degraded.

*Results for Degraded, Non-Degraded, & Standard PE Groups*

There was a significant difference between the mean carbonyl indices for the PE Standards and the PE beach sample groups. Within the PE beach sample groups, no significant difference was observed between beach samples marked absent for visible outside weathering and beach samples marked present for visible outside weathering. As a result of low power calculations, sampling more Non-Degraded PE beach samples is recommended for future studies.

*PS standard (CI) & PS degraded sample (CI)*

| **Polystyrene (PS) Sample Group** | **Carbonyl Index(CI) Mean** | **Standard Deviation** |
|---|---|---|
| PS Standard | 0.223 | 0.081 |
| PS Degraded | 0.409 | 0.116 |

*T-Test & power calculation PS standard (CI) & PS degraded sample (CI)*

$H_0$: The carbonyl index mean for the PS Degraded sample and PS Standard groups are equal. This assumes that there is no detectable difference between the mean carbonyl peak of the PS Standard (CI) and PS Degraded Sample (CI) groups; both PS groups have experienced equal chemical degradation.

$H_1$: The PS Degraded Sample group has a greater mean carbonyl index than the PS Standard group. This assumes the PS Degraded Sample (CI) group is more chemically degraded than the PS Standard (CI) group.

Welch's two sample t-test using the alternative greater argument was performed in R version 3.5.3 software to determine the difference in the means of carbonyl index peaks for the Degraded Sample (CI) and Standard (CI) polystyrene (PS) groups. A significant relationship was detected (Welch's two sample t-test alternative greater: t = 5.4061, df = 29.494, PS Degraded Sample (CI) sd = 0.116, PS Standard (CI) sd = 0.081, p= <0.001 ), supporting the alternative hypothesis and assuming the PS Degraded Sample (CI) group is more chemically degraded than the PS Standard (CI) group.

A two-sample t-test power calculation with unequal sample sizes and unequal variances

was also performed (PS Degraded Sample (CI) n = 21 , PS Standard (CI) n= 12, delta = 0.186 , sig.level = 0.05, alternative = one.sided, power = 0.99986). This calculation resulted in a high power value supporting that there was a reliable difference detected between the group means.

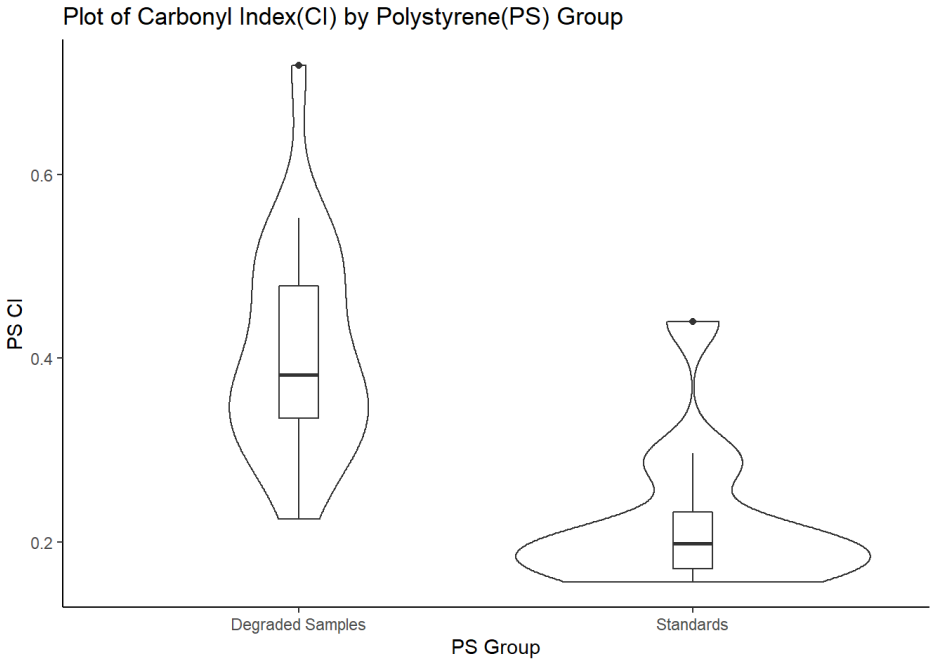


**Figure 9.** Violin plot of carbonyl index (CI) for PS standards and PS degraded samples.

*PS standard (CI) & PS non-degraded sample (CI)*

| **Polystyrene (PS) Sample Group** | **Carbonyl Index(CI) Mean** | **Standard Deviation** |
|---|---|---|
| PS Standard | 0.223 | 0.081 |
| PS Non-Degraded | 0.362 | 0.261 |

*T-Test & power calculation PS standard (CI) & PS non-degraded sample (CI)*

$H_0$: The carbonyl index mean for the PS Non-Degraded sample and PS Standard groups are equal. This assumes that there is no detectable difference between the mean carbonyl peak of the PS Standard (CI) and PS Non-Degraded Sample (CI) groups; both PS groups have experienced equal chemical degradation.

$H_1$: The PS Non-Degraded Sample group has a greater mean carbonyl index than the PS Standard group. This assumes the PS Non-Degraded Sample (CI) group is more chemically degraded than the PS Standard (CI) group.

Welch's two sample t-test using the alternative greater argument was performed in R version 3.5.3 software to determine the difference in the means of carbonyl index peaks for the Non-Degraded Sample (CI) and Standard (CI) polystyrene (PS) groups. No significant relationship was detected (Welch's two sample t-test alternative greater: t = 1.3665, df = 6.6825, PS Non-Degraded Sample (CI) sd = 0.261, PS Standard (CI) sd = 0.081, p = 0.108), resulting in a failure to reject the null hypothesis due to no evidence that the PS Degraded Sample (CI) group is more chemically degraded than the PS Standard (CI) group.

A two-sample t-test power calculation with unequal sample sizes and unequal variances was also performed (PS Non-Degraded Sample (CI) n = 7, PS Standard (CI) n = 12, delta = 0.139, sig.level = 0.05, alternative = one.sided, power = 0.339). This calculation resulted in a low power value supporting that the small sample size limits the detection of a reliable difference between the group means.

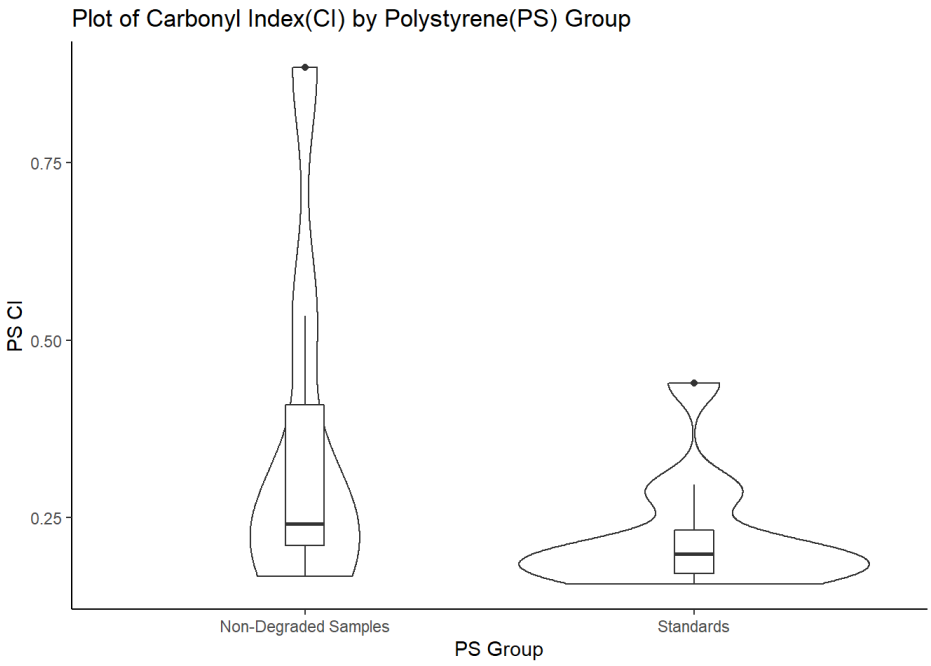


**Figure 10.** Violin plot of carbonyl index (CI) for PS standards and PS non-degraded samples.

*PS non-degraded (CI) & PS degraded sample (CI)*

| **Polystyrene (PS) Sample Group** | **Carbonyl Index(CI) Mean** | **Standard Deviation** |
|---|---|---|
| PS Non-Degraded | 0.362 | 0.261 |
| PS Degraded | 0.409 | 0.116 |

*T-Test & power calculation PS non-degraded (CI) & PS degraded sample (CI)*

$H_0$: The carbonyl index mean for the PS Degraded sample and PS Non-Degraded sample groups are equal. This assumes that there is no detectable difference between the mean carbonyl peak of the PS Degraded Sample (CI) and PS Non-Degraded Sample (CI) groups; both PS groups have experienced equal chemical degradation.

$H_1$: The PS Degraded Sample group has a greater mean carbonyl index than the PS Non-Degraded Sample group. This assumes the PS Degraded Sample (CI) group is more chemically degraded than the PS Non-Degraded Sample (CI) group.

Welch's two sample t-test using the alternative greater argument was performed in R version 3.5.3 software to determine the difference in the means of carbonyl index peaks for the Degraded Sample (CI) and Non-Degraded Sample (CI) polystyrene (PS) groups. No significant relationship was detected (Welch's two sample t-test alternative greater: t = 0.46513, df = 6.7999, PS Degraded Sample (CI) sd = 0.116, PS Non-Degraded Sample (CI) sd = 0.261 , p= 0.328), resulting in a failure to reject the null hypothesis due to no evidence that the PS Degraded Sample (CI) group is more chemically degraded than the PS Non-Degraded Sample (CI) group.

A two-sample t-test power calculation with unequal sample sizes and unequal variances was also performed (PS Degraded (CI) n = 21, PS Non-Degraded Sample (CI) n = 7, delta = 0.047, sig.level = 0.05, alternative = one.sided, power = 0.110). This calculation resulted in a low power value supporting that the small sample size limits the detection of a reliable difference between the group means.

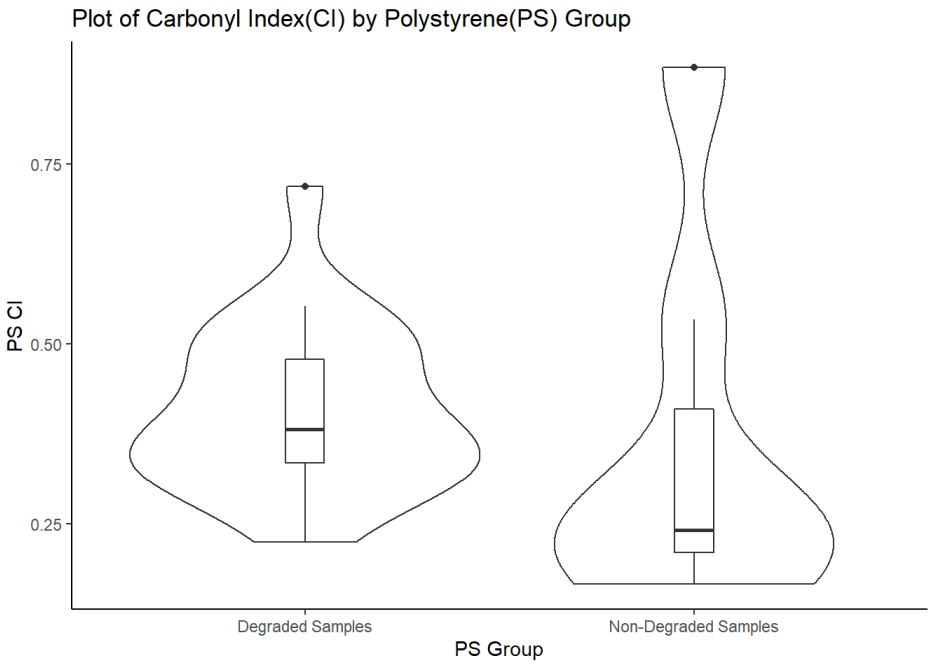


**Figure 11.** Violin plot of carbonyl index (CI) for PS degraded and PS non-degraded samples.

*PS Standard (CI), PS non-degraded (CI), & PS degraded sample (CI) mean plots*

| **PS Standard (CI) Average** | **PS Non-Degraded Sample (CI) Average** | **PS Degraded Sample (CI) Average** |
|---|---|---|
| 0.223 | 0.362 | 0.409 |

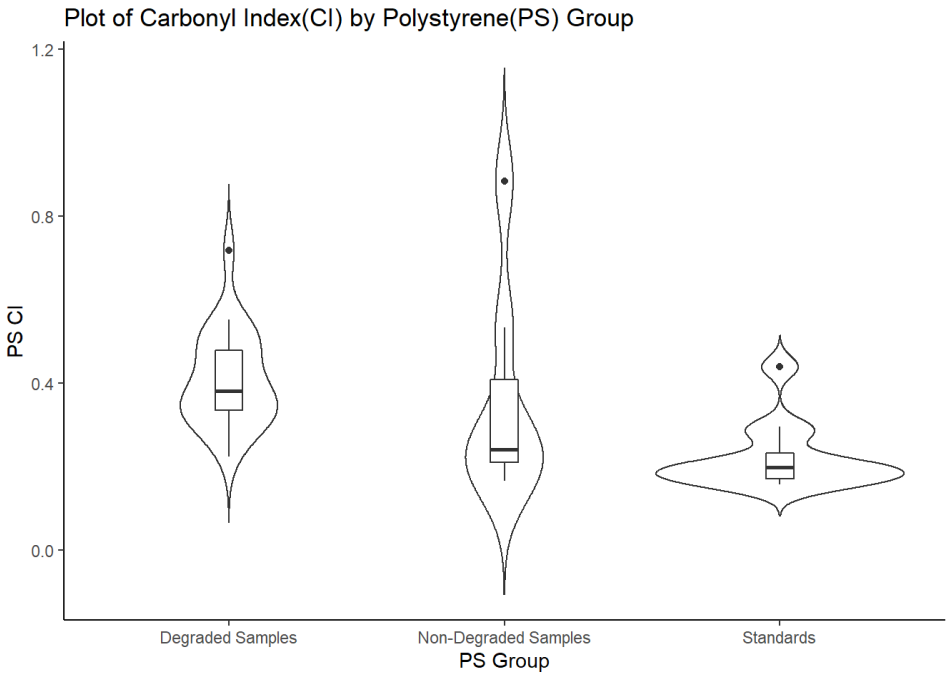


**Figure 12.** Violin plot of carbonyl index (CI) for PS standards, PS non-degraded, and PS degraded samples.

*Results for degraded, non-degraded, & standard PS groups*

There was a significant difference detected between the mean carbonyl indices for the PS Standards and the PS Degraded beach sample groups; supporting a distinguishable relationship between PS Standards and PS beach samples with visible outside weathering. There was no significant difference observed between the mean carbonyl indices for the PS Standards and the PS Non-Degraded beach sample groups. Within the PS beach sample groups, no significant difference was observed between beach samples marked absent for visible outside weathering and PS beach samples marked present for visible outside weathering. As a result of low power calculations, sampling more Non-Degraded PS beach samples is recommended for future studies.

*Final model development*

The multivariate classification algorithm of Principal Component Analysis (PCA) served as the model framework for the final classification tool, and two PCA models were developed and tested. The first PCA model served as a baseline and was built based on the spectra of known unweathered plastic polymers standards. The first PCA model was referred to as the PCA Plastic Polymer Standard Model, which was selected in hypothesis Ⅰ to move forward with the final model development as it separated the 96 standards into eight distinct plastic polymer groups within the modeled 99% confidence limit. The PCA Plastic Polymer Standard Model was evaluated in hypothesis Ⅱ resulting in inside spectra identification being greater than surface spectra identification.

The PCA Plastic Polymer Standard Model was then calibrated with 36 beach plastics' inside spectra including: polyethylene (PE), polystyrene (PS), and polypropylene (PP). The PCA Plastic Polymer Standard & Beach Plastics (PE, PS, & PP) Model Plot (Fig. 13) did not meet evaluation requirements, as only the polyethylene terephthalate (PET) class was separated in the first two principal components and a portion of the PET class was outside the model's overall confident limit.

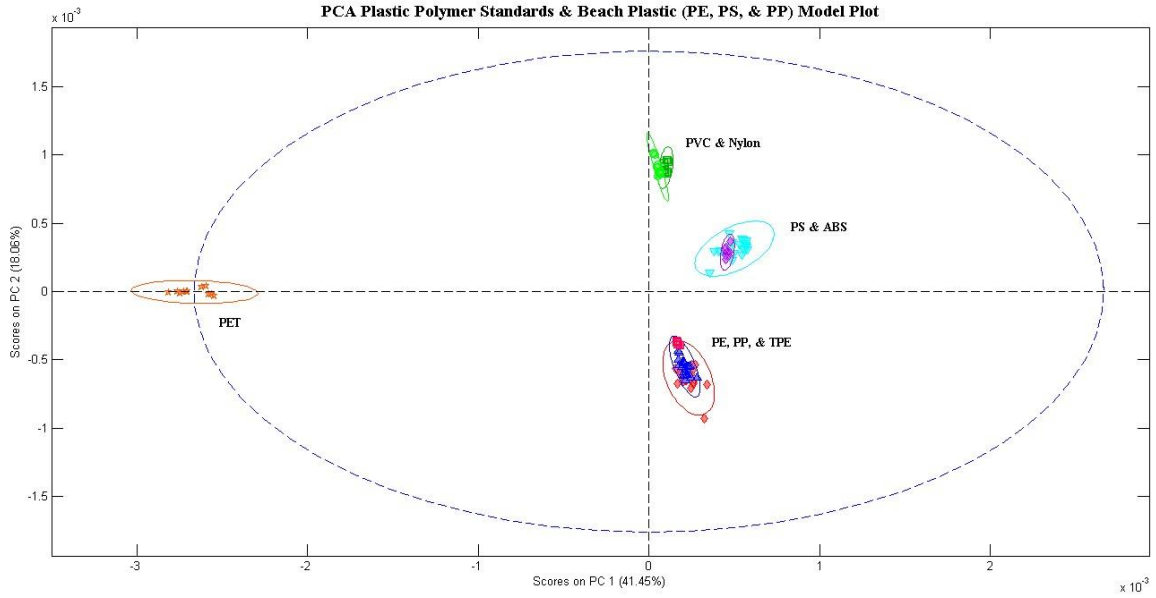


**Figure 13.** The PCA Plastic Polymer Standard & Beach Plastics (PE, PS, & PP) Model Plot was built from all 96 plastic polymer standards inside spectra and 36 beach plastics inside spectra including: polyethylene (PE), polystyrene (PS), and polypropylene (PP), totaling 132 plastics. The overall confidence limit for both models and their confidence ellipse limits, that outlined each class, was set to 99%. The PC 1 & PC 2 scores captured 59.51% of the variance. Prepared in MATLAB version R2017b software and PLS Toolbox 8.6.1 software.

*Plastic polymer class reduction*

As a result of the newly calibrated model not meeting evaluation criteria and resulting in separation difficulties of the plastic polymer clusters in the PC 1 and PC 2 model plots, the PCA Plastic Polymer Standard & Beach Plastics (PE, PS, & PP) Model was then modified to reduce the number of plastic polymer standards and beach plastic spectra to the three most common beach plastic types sampled. The reduced calibrated model was built with an equal number of standards and beach sample spectra for the polyethylene (PE), polypropylene (PP), and polystyrene (PS) classes. Thirty-six identified beach plastic polymer sample spectra (12 beach sample spectra for each polymer type) were calibrated into the model. This procedure was

performed to insure that the beach plastic samples had equal weight to the known plastic polymer standards in the PCA Plastic Polymer Standards Reduced & Beach Plastics (PE, PS, & PP) Model (Fig. 14**)**. Each plastic polymer cluster's confidence ellipse and the overall confidence limit was set to 99%. The PC 1 & PC 2 scores captured 91.6% of the variance.

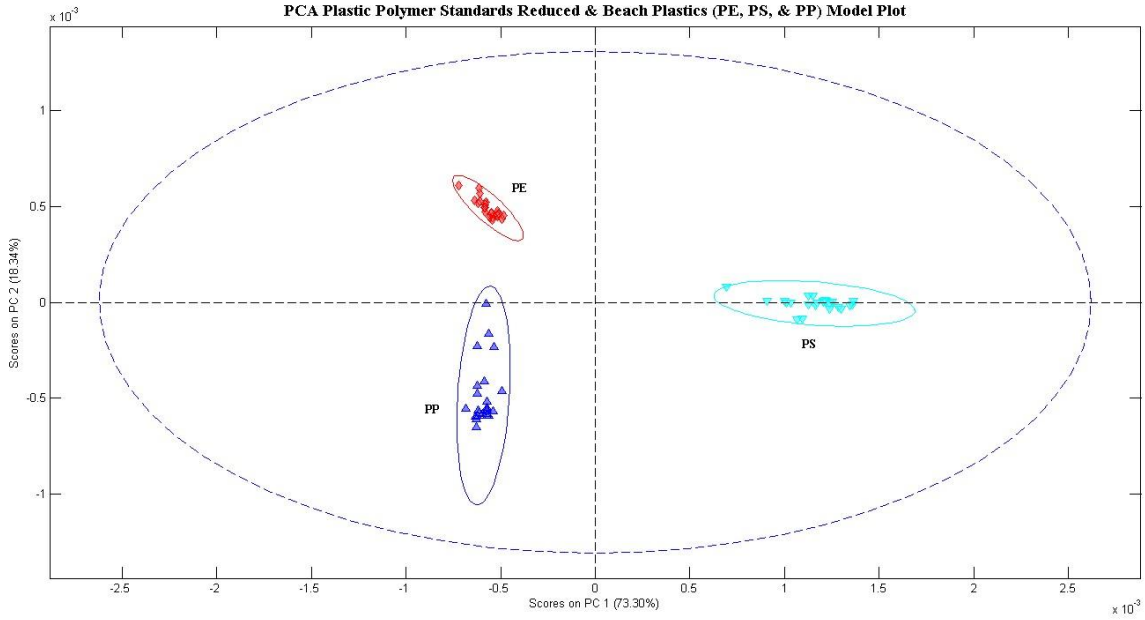


**Figure 14.** The PCA Plastic Polymer Standards Reduced & Beach Plastics (PE, PS, & PP) Model Plot was built from an equal number of plastic polymer standards inside spectra and beach plastics inside spectra. In this model the plastic polymer classes were reduced from eight classes to three classes, to include only polyethylene (PE), polystyrene (PS), and polypropylene (PP). There are 12 plastic polymer standards and 12 beach plastic spectra for each class, totaling 72 plastic spectra for the model. The PCA Plastic Polymer Standards Reduced & Beach Plastics (PE, PS, & PP) Model Plot separated the plastic polymer classes into three distinct clusters; creating a 99% confidence ellipse each cluster, while keeping the classes within the model's overall 99% confidence limit. Prepared in MATLAB version R2017b software and PLS Toolbox 8.6.1 software.

*Beach plastic sample spectra classification - Kona Airport*

As a result of polyethylene (PE), polystyrene (PS), and polypropylene (PP) dominating the beach plastic sampling and the favorable evaluation results of the reduced plastic polymer

model, the PCA Plastic Polymer Standards Reduced & Beach Plastics (PE, PS, & PP) Model was selected for the beach classification process.

Fifty Kona Airport beach sample spectra were applied to the PCA Plastic Polymer Standards Reduced & Beach Plastics Model Plot (Fig. 15). Thirty-nine Kona Airport beach sample spectra fell within a polymer class, and 11 beach sample spectra fell outside the three plastic polymer classes.

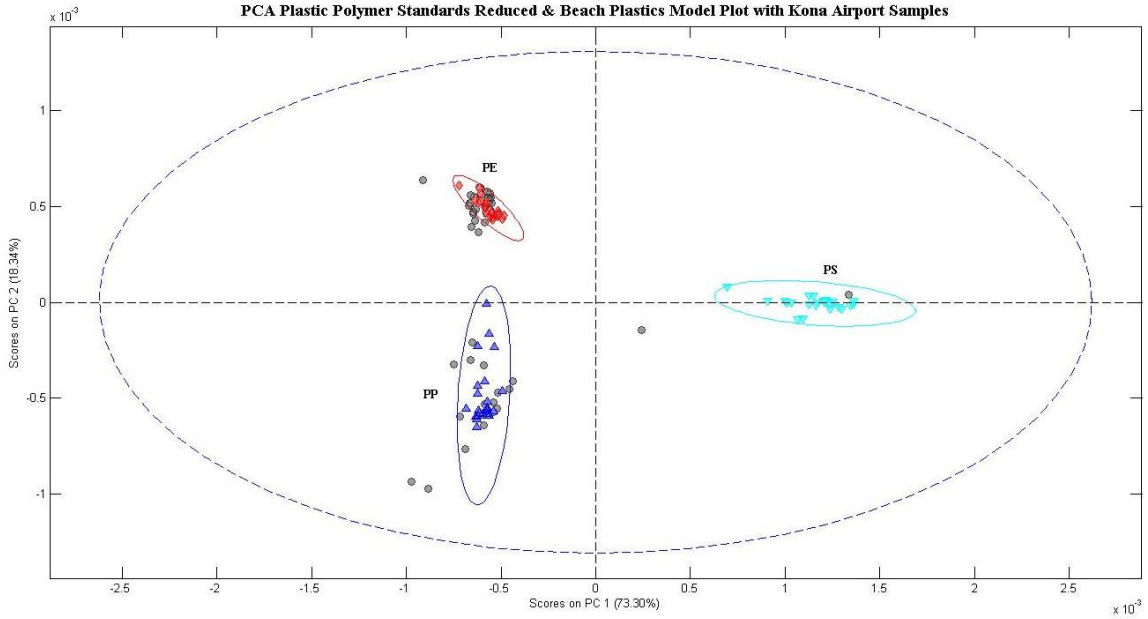


**Figure 15.** PCA Plastic Polymer Standards Reduced & Beach Plastics Model Plot with the addition of 50 Kona Airport sample spectra. The grey dots represent the Kona Airport beach sample spectra that were applied for validation. Thirty-nine sample spectra were classified in the model plot, while 11 were unclassified. Prepared in MATLAB version R2017b software and PLS Toolbox 8.6.1 software.

*Plastic polymer standard classes applied - Kona Airport*

The other five plastic polymer Standard classes of polyethylene terephthalate (PET), polyvinyl chloride (PVC), nylon (nylon), acrylonitrile butadiene styrene (ABS), and

thermoplastic elastomer (TPE) were laid on top of the PCA Plastic Polymer Standards Reduced & Beach Plastics (PE, PS, & PP) Model Plot to build the final Calibrated Model classification tool (Fig. 16). Only Standard spectra were applied to the plot, totaling 60 additional spectra; no beach sample spectra were calibrated into the five Standard classes.

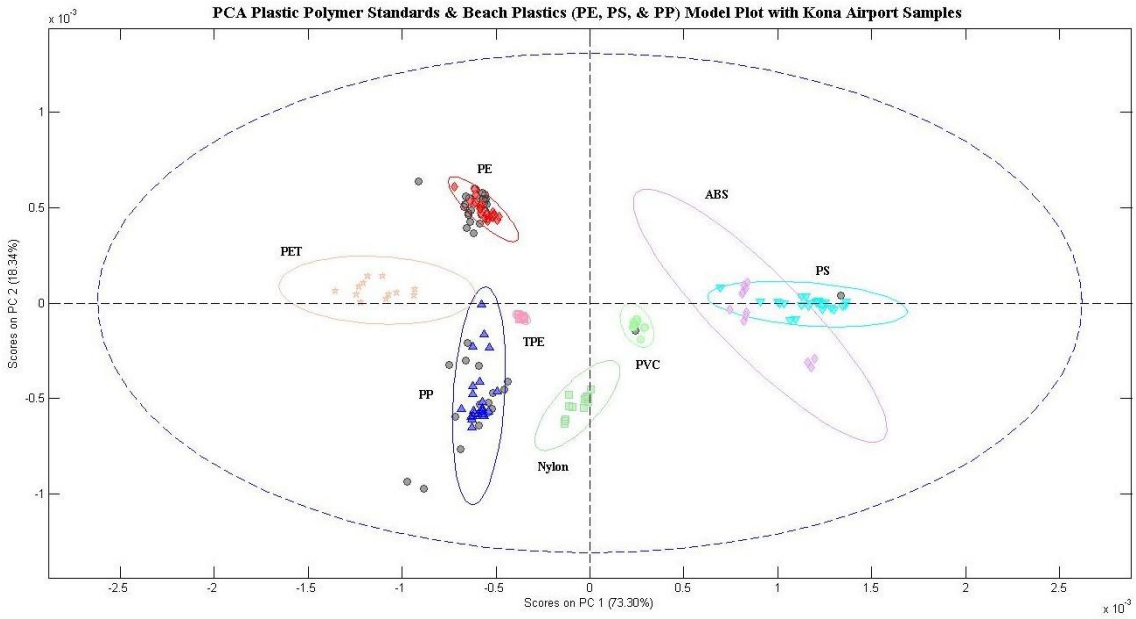


**Figure 16.** PCA Plastic Polymer Standards & Beach Plastics (PE, PS, & PP) Model Plot with Kona Airport Samples. The additional five plastic polymer Standard classes of polyethylene terephthalate (PET), polyvinyl chloride (PVC), nylon (nylon), acrylonitrile butadiene styrene (ABS), and thermoplastic elastomer (TPE) were laid on top of the model. Prepared in MATLAB version R2017b software and PLS Toolbox 8.6.1 software.

*Model classification totals - Kona Airport*

The final Calibrated Model classified 40 out of the 50 beach plastic spectra samples from Kona Airport. An Unknown Kona Airport beach sample spectra became classified as polyvinyl chloride (PVC). The newly classified PVC spectra sample was marked as Unknown by the

Transmittance Band Identification Method. The spectra sample was marked unknown by the Transmittance Band Identification Method as a result of the spectra missing one of five identification bands.

When comparing the models, the Standard Model classified 24 beach plastic spectra and the final Calibrated Model classified 40 beach plastic spectra samples. The Transmittance Band Identification Method, classified all 50 Kona Airport beach plastic spectra samples, including the one Unknown that the Calibrated Model model classified as PVC (Tab. 14).

**Table 14.** The Kona Airport plastic polymer classification breakdown by model/method. The Standard Model, Calibrated Model, and Transmittance Band Identification Method compared.

| **Kona Airport** | *Standard Model* | *Calibrated Model* | *Transmittance Band ID Method* |
|---|---|---|---|
| PE | 19 | 27 | 32 |
| PP | 4 | 11 | 16 |
| PS | 1 | 1 | 1 |
| PVC | 0 | 1 | 0 |
| Unknown | - | - | 1 |
| **Total Plastics ID** | **24** | **40** | **50** |

*Beach plastic sample spectra classification - Hilo Bay*

The same modeling procedure was completed with the Hilo Bay beach plastic spectra samples. Fifty Hilo Bay beach sample spectra were applied to the PCA Plastic Polymer Standards Reduced & Beach Plastics Model Plot (Fig. 17). Thirty-two Hilo Bay beach sample spectra fell within a polymer class, and 18 beach sample spectra fell outside the three plastic

polymer classes.

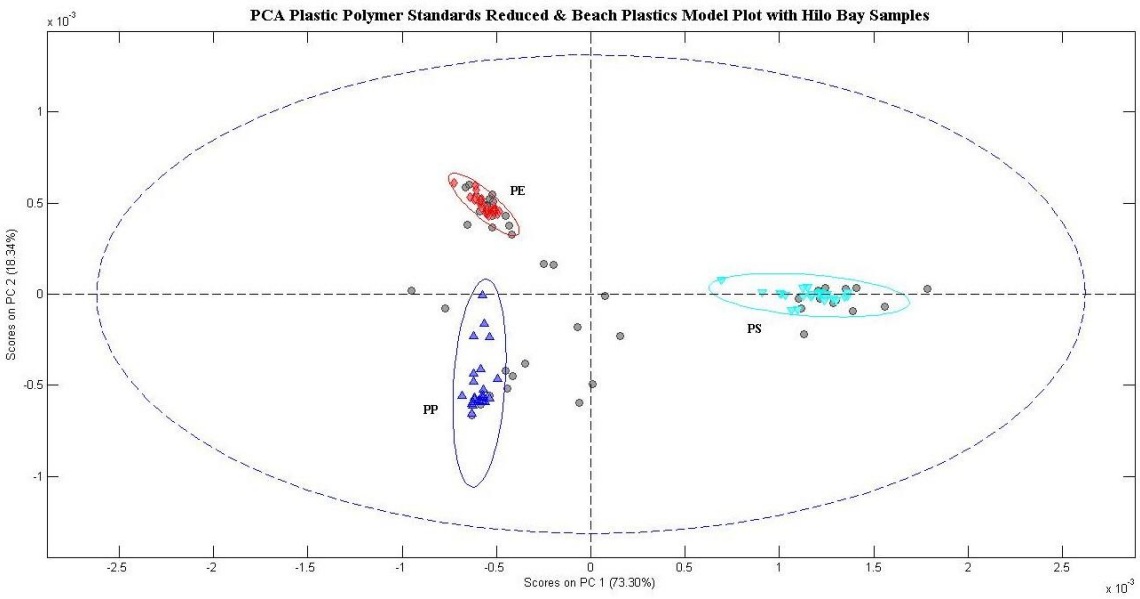


**Figure 17.** PCA Plastic Polymer Standards Reduced & Beach Plastics Model Plot with the addition of 50 Hilo Bay sample spectra. The grey dots represent the Hilo Bay beach sample spectra that were applied for validation. Thirty-two sample spectra were classified in the model plot, while 18 were unclassified. Prepared in MATLAB version R2017b software and PLS Toolbox 8.6.1 software.

*Plastic polymer standard classes applied - Hilo Bay*

The other five plastic polymer Standard classes were again laid on top of the PCA Plastic Polymer Standards Reduced & Beach Plastics (PE, PS, & PP) Model Plot (Fig. 18). The overall confidence limit for the model and each cluster's confidence ellipse limit was again set to 99%. The plastic polymer clusters in the first and second Principal Component Score plot were separated, except for polystyrene (PS) and acrylonitrile butadiene styrene (ABS). There was a distinct overlap between PS and ABS classes.

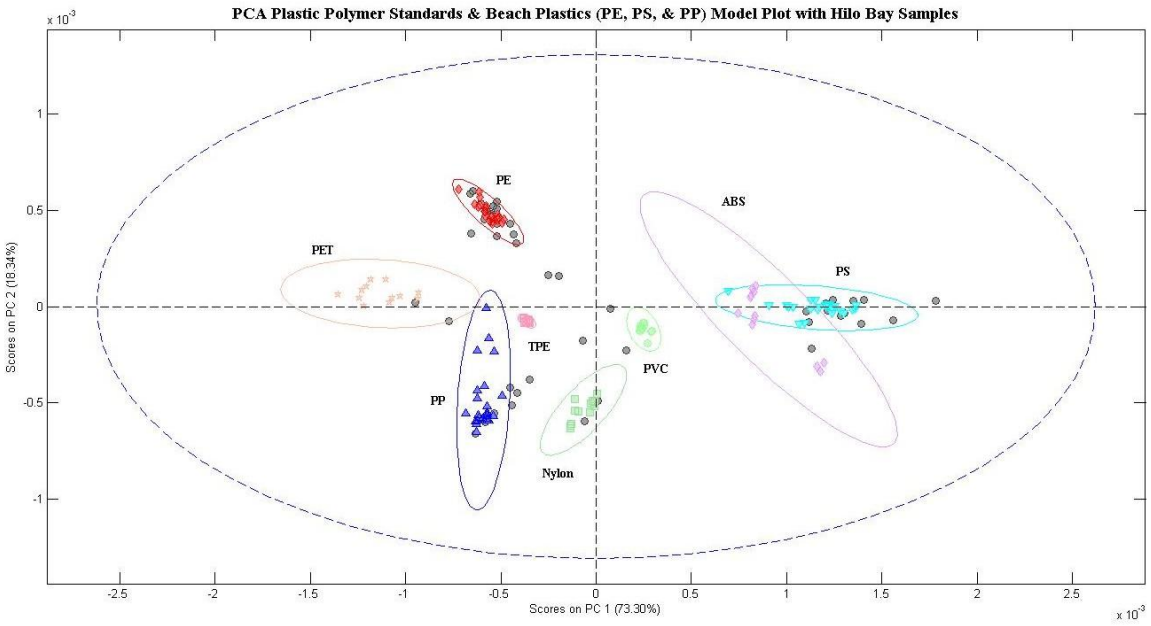


**Figure 18.** PCA Plastic Polymer Standards & Beach Plastics (PE, PS, & PP) Model Plot with Hilo Bay Samples. The additional five plastic polymer Standard classes of polyethylene terephthalate (PET), polyvinyl chloride (PVC), nylon (nylon), acrylonitrile butadiene styrene (ABS), and thermoplastic elastomer (TPE) were laid on top of the model. Prepared in MATLAB version R2017b software and PLS Toolbox 8.6.1 software.

*Model classification totals - Hilo Bay*

The final Calibrated Model classified 37 of the 50 beach plastic spectra samples from Hilo Bay. A total of five Unknown Hilo Bay beach sample spectra were classified. Two Unknown spectra were classified as Nylon, two as polyethylene terephthalate (PET), and one as acrylonitrile butadiene styrene (ABS). The Standard Model classified a total of 18 beach plastic sample spectra, and the Transmittance Band ID Method classified all 50 spectra samples, including four Unknowns (Tab. 15).

**Table 15.** The Hilo Bay plastic polymer classification breakdown by model/method. The Standard Model, Calibrated Model, and Transmittance Band Identification Method compared.

| **Hilo Bay** | *Old Model* | *New Model* | *Transmittance Band ID Method* |
|---|---|---|---|
| PE | 8 | 17 | 20 |
| PP | 1 | 4 | 8 |
| PS | 8 | 11 | 13 |
| PET | 1 | 2 | 3 |
| Nylon | 0 | 2 | 2 |
| ABS | 0 | 1 | 0 |
| Unknown | - | - | 4 |
| **Total Plastics ID** | **18** | **37** | **50** |

*Identification results - Hilo Bay*

The Calibrated Model classified two polyethylene (PE) spectra samples marked as Unknown by the Transmittance Band Identification Method. The PE samples were marked Unknown by the Transmittance Band Identification Method as a result of the spectra missing two of five identification bands.

After examination of the sample spectrum that the Calibrated Model classified as ABS, it appeared that the ABS sample spectrum sample was misidentified by the model. The ABS sample was previously marked a Polystyrene (PS) by the Transmittance Band Identification Method, as a result of all five transmittance bands being present. The overlap between PS and ABS classes on the Calibrated Model Plot most likely contributed to this error.

*Final classification tool model results*

Out of the 100 evaluated beach plastic inside spectra samples, 95 were identified by the Transmittance Band Identification Method (excluding five Unknowns), 77 spectra were identified by the Calibrated Model, and 42 spectra were identified by the Standard Model (Tab. 16). The Calibrated Model not only classified 35 more beach spectra than the Standard Model, it also classified three beach spectra that were marked Unknown by the Transmittance Band Identification Method. However, the Calibrated Model also misclassified one sample.

**Table 16.** The total plastic polymer classification breakdown by model/method. The Standard Model, Calibrated Model, and Transmittance Band Identification Method compared.

| *Standard Model Total* | *Calibrated Model Total* | *Transmittance Band ID Method* | *Beach Plastic Sample Total* |
|---|---|---|---|
| 42 | 77 | 95 | 100 |

It is important to note that the remaining plastic polymer types, which were identified as Unknown, could be strongly chemically degraded common plastic polymer types (> 1 on the carbonyl index) that have fallen outside the 99% confidence ellipses. Unknowns could also be copolymers, contain detectable amounts of additives and/or plasticizers, or may be other plastic polymer types than what was included in the model.

**Discussion**

As a result of numerous metrics and preprocessing applications, developing a robust classification tool for common beach plastic spectra identification remains a challenge. The final beach plastic identification tool, referred to as the Calibrated Model, identified 77% of all beach plastic spectra samples tested. Overall the Calibrated Model classified a greater number of beach plastic sample spectra than the Standard Model. Transmittance Band Identification Method identified a greater number of beach plastic sample spectra than either model. The Transmittance Band Identification Method in combination with the Calibrated Model demonstrated the greatest promise for future studies, as the model and method were able to supervise one another and collectively identify Unknown plastic polymer types.

As a result of the inside beach plastic sample spectra identification being significantly greater than surface beach plastic sample spectra identification, it appears evident that a form of degradation (physical and/or chemical) was taking place on the surface of the beach plastic samples. This degradation on the surface of the samples was negatively affecting the ability of the model to identify beach plastic.

Although there were significant differences detected between the mean Standard (CI) and mean Degraded Beach Sample (CI) spectra for Polyethylene (PE) and Polystyrene (PS), there were no significant differences observed in the mean carbonyl indices of the surface spectra in the beach plastics marked present for visible outside weathering and plastics marked absent for both PE and PS spectra samples.

The Carbonyl Index (CI) method for Polyethylene (PE) that was tested in hypothesis Ⅲ (Focke et al. 2011, Benítez et al. 2013), was determined by Almond et al. 2020 to be incapable of

differentiating significant changes in the evolution of photo-oxidation over time. This may explain why no significant difference was observed. Almond et al. 2020 supports the specified area under band (SAUB) method, as the most effective measurement of determining the CI.

**CI of PE =** Area under the band **1850–1650 $cm^{-1}$** / Area under the band **1500–1420 $cm^{-1}$**

- 1850–1650 $cm^{-1}$ = Area of the carbonyl group (C=O)
- 1500–1420 $cm^{-1}$ = Area of methylene ($CH_2$) reference peak

Almond et al. 2020 calculated the CI for PE by taking the ratio of the area between 1850 to 1650 $cm^{-1}$ and the area of 1850 to 1650 $cm^{-1}$. The area under the band was calculated in absorbance mode with Omnic software using the peak analysis tool (Almond et al. 2020). The SAUB method appears advantageous as it covers a greater wavenumber range, which accounts for a shifting carbonyl peak and a slightly varied, stable reference peak.

Overall, more research is needed to understand the chemical mechanisms of degradation and time in the environment. Future plastic weathering experiments, such as controlled ultraviolet light and seawater exposure coupled with spectra monitoring, is recommended.

We are in the age of plastic. Plastic marine debris is ubiquitous on our beaches and coastlines and in our ocean. This debris has lasting impacts on marine life and ecosystems around the globe (Carson et al. 2013, Clukey et al. 2017). Plastic removal and plastic identification solutions are needed. The Fourier-transform infrared (FT-IR) spectroscopy classification tool developed from this research, coupled with a greater understanding of the degradation process, would allow us to gain insights into potential sources of plastic pollution.

This information could be used to capture plastic waste before it becomes marine debris and prioritize waste removal, and recycling efforts. Through continued, collaborative scientific research we can further our knowledge, conserve natural resources, advance world health, advise policymakers, and alleviate our worldwide plastic pollution pandemic.

**Literature Cited**

Almond, J., P. Sugumaar, M. Wenzel, G. Hill, and C. Wallis. 2020. Determination of the carbonyl index of polyethylene and polypropylene using specified area under band methodology with ATR-FTIR spectroscopy. e-Polymers, 20(1): 369-381.

Andrady, A.L. 1990. Environmental degradation of plastics under land and marine exposure conditions. In: Shomura, R.S. and M.L. Godfrey (eds) Proceedings of the Second International Conference on Marine Debris 848-869.

Andrady, A.L., J.E. Pegram, and S. Nakatsuka. 1993. Changes in carbonyl index and average molecular weight on embrittlement of enhanced photo-degradable polyethylene. Journal of Polymers and the Environment 1(3):171-179.

Barnes, D.K.A., F. Galgani, R.C. Thompson, and M. Barlaz. 2009. Accumulation and fragmentation of plastic debris in global environments. Philosophical Transactions of the Royal Society of London. Series B, Biological sciences 364(1526):1985.

Bejgarn, S., M. Macleod, C. Bogdal, and M. Breitholtz. 2015. Toxicity of leachate from weathering plastics: An exploratory screening study with Nitocra spinipes. Chemosphere 132:114-119.

Benítez, A., J.J Sánchez, M.L. Arnal, A.J. Müller, O. Rodríguez, G. Morales. 2013. Abiotic degradation of LDPE and LLDPE formulated with a pro-oxidant additive. Polymer Degradation and Stability 98:490–501.

Carson, H.S., S.L. Colbert, M.J. Kaylor, and K. J. McDermid. 2011. Small plastic debris changes water movement and heat transfer through beach sediments. Marine Pollution Bulletin 62(8):1708-1713.

Carson, H.S. 2013. The incidence of plastic ingestion by fishes: From the prey's perspective. Marine Pollution Bulletin 74(1):170-174.

Carson, H.S., M.S. Nerheim, K.A. Carroll, and M. Eriksen. 2013. The plastic-associated microorganisms of the North Pacific Gyre. Marine Pollution Bulletin 75(1-2):126-132.

Carson, H.S., M.R. Lamson, D. Nakashima, D. Toloumu, J. Hafner, N. Maximenko, K.J. McDermid. 2013. Tracking the sources and sinks of local marine debris in Hawai'i. Marine Environmental Research 84:76-83.

Chu, Y, A.M. Meyers, B. Wang, W. Yang, J. Jung, and C.F.M. Coimbra. 2015. A sustainable substitute for ivory: The jarina seed from the Amazon. Scientific Reports 5:14387.

Clukey, K.E., C.A. Lepczyk, G.H. Balazs, T.M. Work, and J.M. Lynch. 2017. Investigation of plastic debris ingestion by four species of sea turtles collected as bycatch in pelagic Pacific longline fisheries. Marine Pollution Bulletin 120(1-2):117-125.

Corcoran, P.L., M.C. Biesinger, and M. Grifi. 2009. Plastics and beaches: A degrading relationship. Marine Pollution Bulletin 58:80-84

Costa, M, d.S. Ivar, J. Silva-Cavalcanti, M. Araújo, Â. Spengler, and P. Tourinho. 2010. On the importance of size of plastic fragments and pellets on the strandline: A snapshot of a Brazilian beach. Environmental Monitoring and Assessment 168:299-304.

Endo, S., R. Takizawa, K. Okuda, H. Takada, K. Chiba, H. Kanehiro, H. Ogi, R. Yamashita, and T. Date. 2005. Concentration of polychlorinated biphenyls (PCBs) in beached resin pellets: Variability among individual particles and regional differences. Marine Pollution Bulletin 52: 1103-1114.

Eriksen, M., C.M.L. Laurent, S.C. Henry, M. Thiel, J.M. Charles, C.B. Jose, F. Galgani, G.R. Peter, and J. Reisser. 2014. Plastic pollution in the world's oceans: More than 5 trillion plastic pieces weighing over 250,000 tons afloat at sea. PLOS ONE 9(12):e111913.

Focke, W.W., R.P. Mashele, and NS. Nhlapo. 2011. Stabilization of low-density polyethylene films containing metal stearates as photodegradants. Journal of Vinyl and Additive Technology 17:21-7.

Fotopoulou, K.N., and H.K. Karapanagioti. 2012. Surface properties of beached plastic pellets. Marine Environmental Research 81:70-77.

Fotopoulou, K.N, and H.K Karapanagioti. 2015. Surface properties of beached plastics. Environmental Science and Pollution Research 22(14):11022-11032.

Gewert, B., M. M. Plassmann, and M. MacLeod. 2015. Pathways for degradation of plastic polymers floating in the marine environment. Environmental Science 17(9):1513-1521.

Geyer, R., J. R. Jambeck, and K. L. Law. 2017. Production, use, and fate of all plastics ever made. Science Advances 3(7):e1700782.

Gregory, M.R. 2009. Environmental implications of plastic debris in marine settings--entanglement, ingestion, smothering, hangers-on, hitch-hiking and alien invasions. Philosophical Transactions of the Royal Society of London.Series B, Biological sciences 364(1526):2013.

Hamad, M. L., K. Bowman, N. Smith, X. Sheng, and K. R. Morris. 2010. Multi-scale pharmaceutical process understanding: From particle to powder to dosage form. Chemical Engineering Science 65(21):5625-5638.

Haware, R.V., P. R. Wright, K.R. Morris, and M.L. Hamad. 2011. Data fusion of Fourier transform infrared spectra and powder X- ray diffraction patterns for pharmaceutical mixtures. Journal of Pharmaceutical and Biomedical Analysis 56(5):944-949.

Jambeck, J.R., R. Geyer, C. Wilcox, T.R. Siegler, M. Perryman, A. Andrady, R. Narayan, K.L. Law. 2015. Plastic waste inputs from land into the ocean. Science 347(6223):768

Jayasiri, H., C. Purushothaman, and A. Vennila. 2013. Plastic litter accumulation on high-water strandline of urban beaches in Mumbai, India. Environmental Monitoring and Assessment 185:7709-7719.

Jia, Y., P.H.R. Calil, E.P. Chassignet, E.J. Metzger, J.T. Potemra, K.J. Richards, and A.J. Wallcraft. 2011. Generation of mesoscale eddies in the lee of the Hawaiian Islands. Journal of Geophysical Research: Biogeosciences 116:11.

Jung, M.R., F.D. Horgen, S.V. Orski, C.V. Rodriguez, K.L. Beers, G.H. Balazs, T.T Jones, T.M. Work, K.C. Brignac, S. Royer, K.D. Hyrenbach, B.A, Jensen, and J.M. Lynch. 2018. Validation of ATR FT-IR to identify polymers of plastic marine debris, including those ingested by marine organisms. Marine Pollution Bulletin 127:704-716.

Kiatkamjornwong, S., M. Sonsuk, S. Wittayapichet, P. Prasassarakich, and P. Vejjanukroh. 1999. Degradation of styrene-g-cassava starch filled polystyrene plastics. Polymer Degradation and Stability 66(3):323-335.

Lares, M., M.C. Ncibi, M. Sillanpää, and M. Sillanpää. 2019. Intercomparison study on commonly used methods to determine microplastics in wastewater and sludge samples. Environmental Science and Pollution Research 142:1-14.

Lebreton, L., B. Slat, F. Ferrari, B. Sainte-Rose, J. Aitken, R. Marthouse, S. Hajbane, S. Cunsolo, A. Schwarz, A. Levivier, K. Noble, P. Debeljak, H. Maral, R. Schoeneich-Argent, R. Brambini, and J. Reisser. 2018. Evidence that the Great Pacific Garbage Patch is rapidly accumulating plastic. Scientific Reports 8:4666.

McDermid, K. J., and T. L. McMullen. 2004. Quantitative analysis of small-plastic debris on beaches in the Hawaiian archipelago. Marine Pollution Bulletin 48(7):790-794.

Munari, C., V. Infantini, M. Scoponi, E. Rastelli, C. Corinaldesi, and M. Mistri. 2017. Microplastics in the sediments of Terra Nova Bay (Ross Sea, Antarctica). Marine Pollution Bulletin 122(1-2):161-165.

Rochman, C. M., E. Hoh, B. T. Hentschel, and S. Kaye. 2013. Long-term field measurement of sorption of organic contaminants to five types of plastic pellets: Implications for plastic marine debris. Environmental Science & Technology 47(3):1646.

Royer, S., S. Ferron, S.T. Wilson, D.M. Karl. 2018. Production of methane and ethylene from plastic in the environment. Plos One 13:e0200574.

Satoto, R., W. S. Subowo, R. Yusiasih, Y. Takane, Y. Watanabe, and T. Hatakeyama. 1997. Weathering of high-density polyethylene in different latitudes. Polymer Degradation and Stability 56(3): 275-279.

Shim, W.J., S.H. Hong, S. Eo. 2018. Chapter 1 - Marine microplastics: Abundance, distribution, and composition. In: Zeng EY (ed) Microplastic Contamination in Aquatic Environments: An Emerging Matter of Environmental Urgency. Elsevier, Cambridge, MA 1-26.

Syakti, A. D., R. Bouhroum, N. V. Hidayati, C. J. Koenawan, A. Boulkamh, I. Sulistyo, S. Lebarillier, S. Akhlus, P. Doumenq, and P. Wong-Wah-Chung. 2017. Beach macro-litter monitoring and floating microplastic in a coastal area of Indonesia. Marine Pollution Bulletin 122(1-2):217-225.

Verleye, G.A., N.P. Roeges, and M.O. De Moor. 2001. Easy Identification of Plastics and Rubbers. Rapra Technology Limited, Shropshire, UK. pp. 174.

Young, A.M., and J.A. Elliott. 2016. Characterization of microplastic and mesoplastic debris in sediments from Kamilo Beach and Kahuku Beach, Hawai'i. Marine Pollution Bulletin 113(1):477- 482.

Yousif, E., and R. Haddad. 2013. Photodegradation and photostabilization of polymers, especially polystyrene: Review. SpringerPlus 2(1):1-32.